CC-chemokine/CCR5 interactions and exerts potent activity against R5 human immunodeficiency virus type 1 in vitro. J. Virol. **78:**8654–8662.
14. **Maeda, Y., M. Foda, S. Matsushita, and S. Harada.** 2000. Involvement of both the V2 and V3 regions of the CCR5-tropic human immunodeficiency virus type 1 envelope in reduced sensitivity to macrophage inflammatory protein 1α. J. Virol. **74:**1787–1793.
15. **Marozsan, A. J., S. E. Kuhmann, T. Morgan, C. Herrera, E. Rivera-Troche, S. Xu, B. M. Baroudy, J. Strizki, and J. P. Moore.** 2005. Generation and properties of a human immunodeficiency virus type 1 isolate resistant to the small molecule CCR5 inhibitor, SCH-417690 (SCH-D). Virology **338:**182–199.
16. **Moore, J. P., A. Trkola, and T. Dragic.** 1997. Co-receptors for HIV-1 entry. Curr. Opin. Immunol. **9:**551–562.
17. **Moore, J. P., S. G. Kitchen, P. Pugach, and J. A. Zack.** 2004. The CCR5 and CXCR4 coreceptors central to understanding the transmission and pathogenesis of human immunodeficiency virus type 1 infection. AIDS Res. Hum. Retrovir. **20:**111–126.
18. **Nishikawa, M., K. Takashima, T. Nishi, R. A. Furuta, N. Kanzaki, Y. Yamamoto, and J. Fujisawa.** 2005. Analysis of binding sites for the new small-molecule CCR5 antagonist TAK-220 on human CCR5. Antimicrob. Agents Chemother. **49:**4708–4715.
19. **Pierson, T. C., and R. W. Doms.** 2003. HIV-1 entry inhibitors: new targets, novel therapies. Immunol. Lett. **85:**113–118.
20. **Regoes, R. R., and S. Bonhoeffer.** 2005. The HIV coreceptor switch: a population dynamical perspective. Trends Microbiol. **13:**269–277.
21. **Samson, M., F. Libert, B. J. Doranz, J. Rucker, C. Liesnard, C. M. Farber, S. Saragosti, C. Lapoumeroulie, J. Cognaux, C. Forceille, G. Muyldermans, C. Verhofstede, G. Burtonboy, M. Georges, T. Imai, S. Rana, Y. Yi, R. J. Smyth, R. G. Collman, R. W. Doms, G. Vassart, and M. Parmentier.** 1996. Resistance to HIV-1 infection in Caucasian individuals bearing mutant alleles of the CCR-5 chemokine receptor gene. Nature **382:**722–725.
22. **Sato, M., T. Motomura, H. Aramaki, T. Matsuda, M. Yamashita, Y. Ito, H. Kawakami, Y. Matsuzaki, W. Watanabe, K. Yamataka, S. Ikeda, E. Kodama, M. Matsuoka, and H. Shinkai.** 2006. Novel HIV-1 integrase inhibitors derived from quinolone antibiotics. J. Med. Chem. **49:**1506–1508.
23. **Schols, D., S. Struyf, J. Van Damme, J. A. Este, G. Henson, and E. De Clercq.** 1997. Inhibition of T-tropic HIV strains by selective antagonization of the chemokine receptor CXCR4. J. Exp. Med. **186:**1383–1388.
24. **Shioda, T., J. A. Levy, and C. Cheng-Mayer.** 1991. Macrophage and T cell-line tropisms of HIV-1 are determined by specific regions of the envelope gp120 gene. Nature **349:**167–169.
25. **Strizki, J. M., C. Tremblay, S. Xu, L. Wojcik, N. Wagner, W. Gonsiorek, R. W. Hipkin, C.-C. Chou, C. Pugliese-Sivo, Y. Xiao, J. R. Tagat, K. Cox, T. Priestley, S. Sorota, W. Huang, M. Hirsch, G. R. Reyes, and B. M. Baroudy.** 2005. Discovery and characterization of vicriviroc (SCH 417690), a CCR5 antagonist with potent activity against human immunodeficiency virus type 1. Antimicrob. Agents Chemother. **49:**4911–4919.
26. **Strizki, J. M., S. Xu, N. E. Wagner, L. Wojcik, J. Liu, Y. Hou, M. Endres, A. Palani, S. Shapiro, J. W. Clader, W. J. Greenlee, J. R. Tagat, S. McCombie, K. Cox, A. B. Fawzi, C.-C. Chou, C. Pugliese-Sivo, L. Davies, M. E. Moreno, D. D. Ho, A. Trkola, C. A. Stoddart, J. P. Moore, G. R. Reyes, and B. M. Baroudy.** 2001. SCH-C (SCH 351125), an orally bioavailable, small molecule antagonist of the chemokine receptor CCR5, is a potent inhibitor of HIV-1 infection *in vitro* and *in vivo*. Proc. Natl. Acad. Sci. USA **98:**12718–12723.
27. **Takashima, K., H. Miyake, N. Kanzaki, Y. Tagawa, X. Wang, Y. Sugihara, Y. Iizawa, and M. Baba.** 2005. Highly potent inhibition of human immunodeficiency virus type 1 replication by TAK-220, an orally bioavailable small molecule CCR5 antagonist. Antimicrob. Agents Chemother. **49:**3474–3482.
28. **Tremblay, C. L., F. Giguel, T. C. Chou, H. Dong, K. Takashima, and M. S. Hirsch.** 2005. TAK-652, a novel CCR5 inhibitor, has favourable drug interactions with other antiretrovirals in vitro. Antivir. Ther. **10:**967–968.
29. **Trkola, A., S. E. Kuhmann, J. M. Strizki, E. Maxwell, T. Ketas, T. Morgan, P. Pugach, S. Xu, L. Wojcik, J. Tagat, A. Palani, S. Shapiro, J. W. Clader, S. McCombie, G. R. Reyes, B. M. Baroudy, and J. P. Moore.** 2002. HIV-1 escape from a small molecule, CCR5-specific entry inhibitor does not involve CXCR4 use. Proc. Natl. Acad. Sci. USA **99:**395–400.
30. **Tuttle, D. L., C. B. Anders, M. J. Aquino-De Jesus, P. P. Poole, S. L. Lamers, D. R. Briggs, S. M. Pomeroy, L. Alexander, K. W. Peden, W. A. Andiman, J. W. Sleasman, and M. M. Goodenow.** 2002. Increased replication of non-syncytium-inducing HIV type 1 isolates in monocyte-derived macrophages is linked to advanced disease in infected children. AIDS Res. Hum. Retrovir. **18:**353–362.
31. **Yeni, P. G., S. M. Hammer, M. S. Hirsch, M. S. Saag, M. Schechter, C. C. Carpenter, M. A. Fischl, J. M. Gatell, B. G. Gazzard, D. M. Jacobsen, D. A. Katzenstein, J. S. Montaner, D. D. Richman, R. T. Schooley, M. A. Thompson, S. Vella, and P. A. Volberding.** 2004. Treatment for adult HIV infection: 2004 recommendations of the International AIDS Society—USA Panel. JAMA **292:**251–265.

Antiviral Chemistry & Chemotherapy 18:201–211

Potent and selective inhibition of Tat-dependent HIV-1 replication in chronically infected cells by a novel naphthalene derivative JTK-101

Xin Wang[1], Kazunobu Yamataka[1,2], Mika Okamoto[1], Satoru Ikeda[2] and Masanori Baba[1]*

[1]Division of Antiviral Chemotherapy, Center for Chronic Viral Diseases, Graduate School of Medical and Dental Sciences, Kagoshima University, Kagoshima, Japan
[2]Central Pharmaceutical Research Institute, Japan Tobacco Inc., Takatsuki, Japan

*Corresponding author: Tel: +81 99 275 5930; Fax: +81 99 275 5932; E-mail: m-baba@vanilla.ocn.ne.jp

In search for effective human immunodeficiency virus type 1 (HIV-1) transcription inhibitors, we have evaluated more than 100,000 compounds for their inhibitory effects on HIV-1 long terminal repeat (LTR)-driven reporter gene expression, and identified a novel naphthalene derivative, JTK-101. This compound could suppress tumour necrosis factor (TNF)-α-induced HIV-1 production in latently infected OM-10.1 cells at nanomolar concentrations. JTK-101 could also potently inhibit constitutive HIV-1 production in MOTL-4/III$_B$. However, the antiviral activity of JTK-101 was found to be much weaker in acutely infected cells and the chronically infected cells U937/III$_B$ cells than in OM-10.1 and MOLT-4/III$_B$ cells. JTK-101 selectively suppressed TNF-α-induced HIV-1 mRNA synthesis in OM-10.1 cells in a dose-dependent fashion. JTK-101 modestly inhibited TNF-α-induced HIV-1 LTR-driven reporter gene expression, but potently inhibited Tat-induced gene expression. Immunoblot analysis revealed that low-level expression of the Tat cofactors CDK9 and cyclin T1 might contribute to the diminished antiviral activity in U937/III$_B$ cells. Furthermore, JTK-101 could not inhibit HIV-1 replication in chronically infected monocytes/macrophages, in which CDK9 and cyclin T1 were undetectable. These results suggest that JTK-101 exerts its anti-HIV-1 activity through the inhibition of known or unknown Tat cofactors, presumably CDK9/cyclin T1.

Keywords: CDK9/cyclin T1, HIV-1, naphthalene derivative, NF-κB, Tat

Introduction

Significant progress in the treatment of human immunodeficiency virus type 1 (HIV-1) infection has been achieved by the advent of highly active antiretroviral therapy (HAART), which targets different steps in the viral replication cycle with multiple inhibitors (Yeni *et al.*, 2004). At present, one entry inhibitor, eight nucleoside or nucleotide reverse transcriptase inhibitors (NRTIs), three non-NRTIs (NNRTIs) and eight protease inhibitors (PIs) are available for the treatment of HIV-1 infection. HAART with these inhibitors has significantly decreased plasma viraemia to undetectable levels and has considerably improved the survival of infected individuals (Pomerantz & Horn, 2003). However, considering the drug resistance and side effects of long-term HAART, discovery of novel HIV-1 agents with different mechanisms of action is still highly desirable. In addition, the reservoir cells containing latent HIV-1 are capable of producing infectious particles after cellular activation, which leads to a rebound of the viral load after interruption of HAART (Pierson *et al.*, 2000). Therefore, HAART cannot be terminated unless such reservoir cells have been eradicated or viral recovery from the cells can be completely suppressed. In this regard, inhibitors that selectively prevent HIV-1 gene expression can potentially inhibit the recovery of latent virus from resting memory T cells as well as infected monocytes/macrophages (M/Ms), which are also considered to be a long-surviving chronically infected cell population in HIV-1-infected patients.

Molecular analyses of HIV-1 replication have revealed a concerted complexity that regulates the viral life cycle. Among the various steps of the HIV-1 life cycle, transcription from the integrated proviral DNA is considered to be a crucial step for viral replication, as amplification of the viral genetic information is attainable only through transcription (Cullen, 1991; Jones & Peterlin, 1994; Okamoto, 1995). The viral-encoded transactivator protein Tat stimulates transcriptional elongation through its interaction with the transactivation response (TAR) RNA structure. Tat also interacts with cellular cofactors, such as positive transcription elongation factor b (P-TEFb), a complex composed of cyclin T1 and cyclin-dependent

kinase 9 (CDK9; Peng *et al.*, 1998; Price, 2000; Wei *et al.*, 1998). CDK9 hyperphosphorylates the carboxy-terminal domain of RNA polymerase II, and induces efficient promoter clearance and transcriptional elongation. In addition to the viral protein Tat, several cellular factors are known to regulate HIV-1 gene expression (Peterlin & Trono, 2003). Among these factors, nuclear factor κB (NF-κB) is the most potent activator of HIV-1 gene expression (Nobel & Baltimore, 1987). In general, NF-κB exists in an inactive form in the cytoplasm, where it is bound to the inhibitory molecule IκBα. Stimulation of the cells with several cytokines, such as tumour necrosis factor-α (TNF-α), leads to the immediate degradation of IκBα and activates NF-κB, resulting in immediate translocation of NF-κB from the cytoplasm to the nucleus (Roulston *et al.*, 1995). HIV-1 gene expression is initiated and enhanced by the activation of NF-κB and subsequent binding to the specific DNA motifs in the enhancer region of the HIV-1 long terminal repeat (LTR). However, complex and unknown machinery may also be involved in the regulation of HIV-1 gene expression.

Several compounds have been reported to suppress HIV-1 gene expression and replication through the inhibition of Tat or NF-κB. In our previous studies, the fluoroquinoline derivative K-37 proved to be a potent and selective HIV-1 transcription inhibitor in both acutely and chronically infected cells at nanomolar concentrations (Baba *et al.*, 1998). K-37 was an inhibitor of not only Tat but also other RNA-dependent transactivators. Although its target molecule remains to be elucidated, the aminoquinolone WM5, which is structurally related to K-37, was found to interact with the bulge region of the TAR (Parolin *et al.*, 2003; Richter *et al.*, 2004).

In our recent extensive search programme for novel HIV-1 transcription inhibitors, more than 100,000 compounds have been examined for their inhibitory effects on HIV-1 LTR-driven reporter gene expression in cell cultures. Among the test compounds, several compounds showed selective inhibition of HIV-1 replication in chronically infected cells; the novel naphthalene derivative JTK-101 (Figure 1) was selected as the representative of the active compounds because it exhibited the highest selectivity. JTK-101 is a more potent and selective transcription inhibitor of HIV-1 than K-37 in latently and chronically infected cells. Studies of its mechanism of action suggest that JTK-101 is an inhibitor of Tat cofactors, presumably CDK9/cyclin T1.

Materials and methods

Compounds

JTK-101 (Figure 1) was synthesized by Japan Tobacco Co. (Takatsuki, Japan) and the fluoroquinoline derivative K-37 (Figure 1) was provided by Daiichi Pharmaceutical Co.

Figure 1. Chemical structures of JTK-101 and K-37

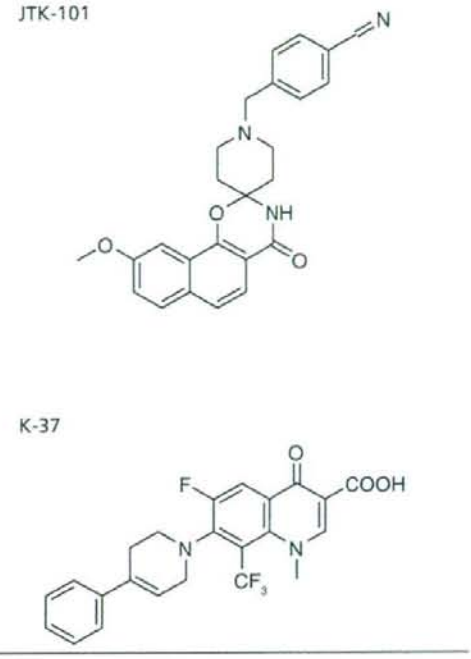

(Tokyo, Japan). Lamivudine (3TC), zidovudine (AZT), and the histone deacetylase inhibitor trichostatin A (TSA) were purchased from Sigma (St. Louis, MO, USA). All compounds were dissolved in DMSO at 10 mM or higher concentrations to exclude any antiviral or cytotoxic effect of DMSO and stored at -20°C until use.

Cells and virus

Peripheral blood mononuclear cells (PBMCs), CEM, MOLT-4, OM-10.1 cells, MOLT-4/III_B, and U937/III_B cells were used in antiviral assays. OM-10.1 cells are a clone of HL-60 cells latently infected with HIV-1. MOLT-4/III_B and U937/III_B cells are MOLT-4 and U937 cells chronically infected with HIV-1 (III_B strain), respectively. PBMCs were obtained from healthy donors and stimulated with phytohaemagglutinin (PHA; Sigma). W-3 and KM-3 cells were clones of CEM cells that stably integrate an HIV-1 LTR-driven secreted alkaline phosphatase (SEAP) gene. The integrated HIV-1 LTR contains two intact NF-κB-binding sites in W-3 cells, whereas both of the sites are mutated in KM-3 cells. M/Ms were isolated from healthy donors and cultivated according to the procedure described previously (Perno *et al.*, 1988). Two strains of HIV-1 (III_B and Ba-L) were used in antiviral assays. III_B and Ba-L are CXCR4- and CCR5-using strains,

respectively. One CCR5-using HIV-1 isolate (CTV), and one CCR5- and CXCR4-using HIV-1 isolate (HE) were also used in antiviral assays.

Antiviral assays

The activities of the compounds against chronic HIV-1 infection were based on the inhibition of HIV-1 p24 antigen production. OM-10.1 cells (1×10^5 cells/ml) were incubated in the absence or presence of the compounds for 2 h and stimulated with 1 ng/ml TNF-α (Boehringer-Mannheim, Mannheim, Germany), whereas MOLT-4/III_B and U937/III_B cells (1×10^5 cells/ml) were cultured in the absence or presence of the test compounds without any stimulation. After 3 days of incubation at 37°C, the culture supernatants were collected and their p24 antigen levels were determined with a sandwich enzyme-linked immunosorbent assay kit (Cellular Products, Buffalo, NY, USA). The cytotoxicity of the test compounds for the chronically infected cells were determined by the 3-(4,5-dimethylthiazol-2-yl)-2,5-diphenyltetrazolium bromide (MTT) method (Pauwels *et al.*, 1988).

The assay procedure for measuring the anti-HIV-1 activity of the compounds in chronically infected M/Ms was also based on the quantitative detection of p24 antigen in the culture supernatants. The isolated M/Ms (5×10^4 cells/ml) were cultured in RPMI 1640 medium supplemented with 10% heat-activated fetal calf serum, 10% heat-inactivated human AB serum, penicillin G (100 U/ml), and streptomycin (100 μg/ml). At day 7, differentiated M/Ms were infected with HIV-$1_{Ba\text{-}L}$ (10 ng of p24 per 5×10^4 cells). After 24 h incubation, the cells were washed and cultured for a further 9 days. After extensive washing, chronically infected M/Ms were cultured in the absence or presence of the test compounds for 4 days without medium change. The culture supernatants were collected and examined for their p24 antigen levels. The cytotoxicity of the test compounds for M/Ms was also determined by the MTT method.

The compounds' activities against acute HIV-1 infection were based on the inhibition of virus-induced cytopathicity in CEM cells and p24 antigen production in PBMCs, as described previously (Baba *et al.*, 1998). CEM cells (1×10^5 cells/ml) were infected with the virus at a multiplicity of infection of 0.01 and cultured in the presence of various concentrations of the compounds. After 4 days of incubation at 37°C, the CEM cells were subcultured at a ratio of 1:5 with fresh culture medium containing appropriate concentrations of the test compounds and further cultured. For the assays in PBMCs, the cells (1×10^5 cells/ml) were infected with HIV-1 at a multiplicity of infection of 0.1. After virus adsorption for 2 h, the cells were extensively washed to remove unadsorbed virus particles and cultured in the presence of various concentrations of the test compounds. After 6 days incubation at 37°C, the culture supernatants were collected and examined for their p24 antigen levels. The cytotoxicity of the test compounds were also determined by the MTT method.

Quantitative RT-PCR analysis

OM-10.1 cells (2.5×10^5 cells/ml) were incubated in the absence or presence of the JTK-101 for 2 h, stimulated with 1 ng/ml TNF-α, and further incubated for 24 h. Total RNA was extracted from the cells with an RNA extraction kit (Promega, Madison, WI, USA). The extracted RNA was subjected to quantitative RT-PCR analysis to determine HIV-1 mRNA, using GeneAmp 5700 Sequence Detection System (Applied Biosystems, Foster City, CA, USA). For quantitative RT-PCR, Taqman One-Step RT-PCR Master Mix Reagents Kit (Applied Biosystems) was used according to the manufacturer's instructions. Using the sequence of the HIV-1 molecular clone HXB2, a primer pair and a probe were designed downstream of the transcription initiation site for HIV-1 mRNA. The primer pairs and the probes were 581F (5′-TGGTAACTAGAGTCCCTCAGACC-3′, nucleotide position 582–605), 683R (5′-AGCTCCTCTG-GTTTCCCTTTC-3′, nucleotide position 662–682) and 620T (5′-TGGAAAATCTCTCTAGCAGTGGCGCC-GAAC-3′, nucleotide position 619–647). Non-specific inhibition of host cellular mRNA synthesis by JTK-101 was determined with Taqman GAPDH Control Reagents kit (Applied Biosystems).

Reporter gene assays

W-3 and KM-3 cells were either treated with 10 ng/ml TNF-α or transfected with 1 μg of plasmid expressing HIV-1 Tat, which contains the second exon under the control of the simian virus 40 promoter (modification of pSV2tat72), by Lipofectamine 2000 (Invitrogen, Carlsbad, CA, USA). The cells were cultured in the presence of various concentrations of the test compounds. After 2 days of incubation at 37°C, the SEAP activities in the culture supernatants were determined by chemiluminescence. The SEAP activities were measured using the GreatEscape SEAP detection kit (CLONTECH, Palo Alto, CA, USA), according to the manufacturer's instructions. The chemiluminescence intensity was measured with a LB96P luminometer (Berthold, Wildbad, Germany). At the same time, the number of viable cells was determined by the MTT method.

Immunoblot analysis

Immunoblot analysis was performed as described previously (Wang *et al.*, 2002). Briefly, cells extracts were prepared by incubating cells in lysis buffer (50 mM Tris [pH 8.0], 120 mM NaCl and 0.5% NP-40) containing protease inhibitor cocktail and phenylmethylsulphonyl fluoride (Sigma, St. Louis, MO, USA). Protein concentra-

Figure 2. Inhibitory effects of JTK-101 and K-37 on HIV-1 replication in TNF-α-stimulated OM-10.1 cells

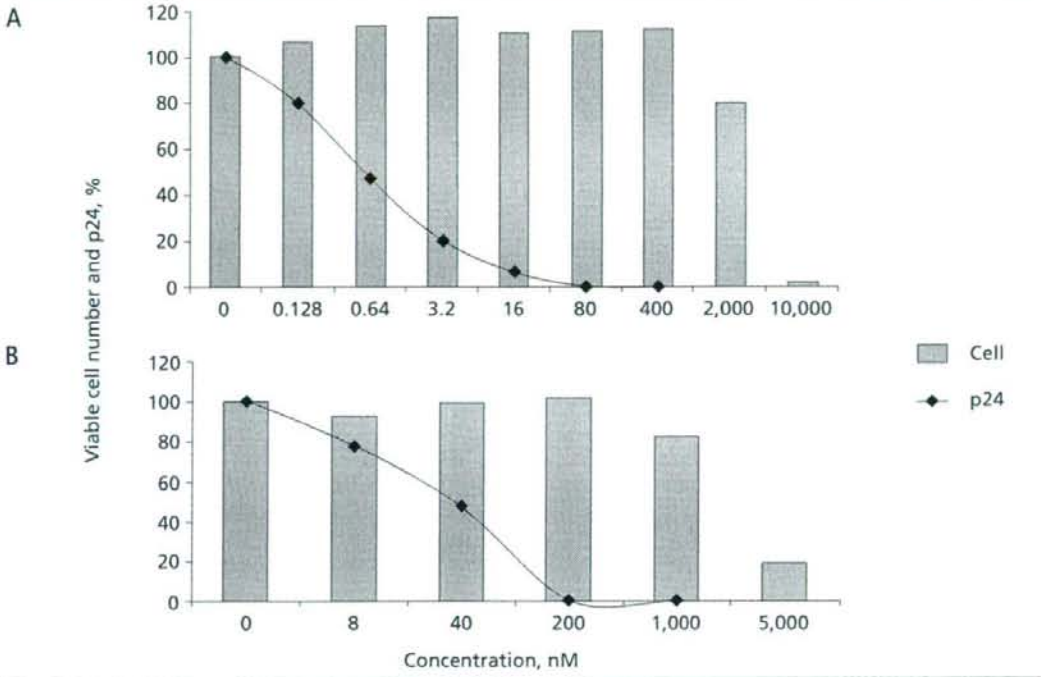

(A) Inhibitory effects of JTK-101. **(B)** Inhibitory effects of K-37. OM-10.1 cells were incubated in the absence or presence of the test compounds for 2 h, stimulated with TNF-α (1 ng/ml), and further incubated. After 3 days of incubation, the p24 antigen levels of culture supernatants (lines) were measured by ELISA. At the same time, the number of viable cell was determined by the 3-(4,5-dimethylthiazol-2-yl)-2,5-diphenyltetrazolium bromide (MTT) method (columns). The experiments were repeated three times and representative results are shown.

tions were determined by Bio-Rad protein assay, and equal amount of total protein was loaded onto 10% sodium dodecyl sulphate-polyacrylamide gels. The immunoblotting procedure using enhanced chemiluminescence for detection was also described previously. CDK9 was detected using a rabbit polyclonal antibody (C-20 sc-484; Santa Cruz Biotechnology, Santa Cruz, CA, USA), Cyclin T1 was detected using a goat polyclonal antibody (T-18 sc-8127; Santa Cruz Biotechnology), and actin was detected with goat polyclonal antibody (C-11 sc-1615; Santa Cruz Biotechnology). Complexes were then detected using an anti-rabbit horseradish peroxidase-conjugated secondary goat antibody and an anti-goat horseradish peroxidase-conjugated secondary rabbit antibody (MP Biomedicals, Aurora, OH, USA), and visualized by enhanced chemiluminescence western blotting detection system (Amersham Biosciences, Buckinghamshire, UK). For chronically infected M/Ms, the isolated M/Ms were kept uninfected or infected with HIV-$1_{Ba\text{-}L}$ (10 ng of p24 per 5×10^4 cells). After chronic infection of M/Ms with HIV-$1_{Ba\text{-}L}$, the M/M cells and culture supernatants were collected on day 17 for cellular extract preparation and p24 antigen detection, respectively. HIV-1 p24 levels in four donors ranged between 30 and 200 ng/ml (data not shown). As a control, PBMCs obtained from the same donors and stimulated with PHA for 3 days were also used for western blot analysis for CDK9 and cyclin T1.

Results

Antiviral activity in chronically infected cell lines

We first evaluated JTK-101 for its inhibitory effects on HIV-1 replication in chronically infected cells. OM-10.1 cells produce little or no HIV-1 under basal conditions, but do produce a significant level of virus after stimulation with TNF-α or phorbol 12-myristate 13-acetate (PMA; Butera *et al.*, 1991). In fact, the level of HIV-1 p24 antigen in culture supernatant was less than 1 ng/ml in unstimulated OM-10.1 cells, yet it reached 100 ng/ml or more after stimulation with 1 ng/ml TNF-α (data not shown). As shown in Figure 2A, JTK-101 suppressed p24 antigen production in

Table 1. Inhibitory effects of JTK-101 and other selected compounds on HIV-1 replication in chronically infected cells*

Compound	Cells	EC_{50}†, μM	CC_{50}‡, μM	SI§
JTK101	OM-10.1	0.0014 ±0.0005	3.8 ±0.2	2,714
	MOLT-4/III_B	0.0057 ±0.0025	1.3 ±0.4	228
K-37	OM-10.1	0.033 ±0.012	2.1 ±0.3	63
	MOLT-4/III_B	0.074 ±0.033	>5.0	>68
3TC	OM-10.1	>20	>20	–
	MOLT-4/III_B	>20	>20	–

*All data represent means ±SD for three separate experiments. †Concentration required for 50% inhibition of p24 antigen production in culture supernatants. ‡Concentration required for 50% inhibition of cell proliferation and viability. §Selectivity index (ratio of CC_{50} to EC_{50}).

TNF-α-stimulated OM-10.1 cells in a dose-dependent fashion. The compound completely prevented p24 antigen production at a concentration of 0.08 μM. However, it did not reduce cell viability and proliferation at a concentration of 2 μM. The EC_{50} and CC_{50} of JTK-101 were 0.0014 and 3.8 μM, respectively. K-37 (Figure 1), another potent HIV-1 transcription inhibitor, could also suppress the production of p24 antigen in a dose-dependent fashion (Figure 2B). The EC_{50} and CC_{50} of K-37 was 0.033 and 2.1 μM, respectively (Table 1). Thus, their selectivity indexes, based on the ratio of their CC_{50}s to EC_{50}s, were 2,714 and 63 for JTK-101 and K-37, respectively, indicating that JTK-101 is a much more potent and selective inhibitor of HIV-1 replication in chronically infected cells than K-37.

The inhibitory effects of JTK-101 on HIV-1 replication were also evaluated in MOLT-4/III_B and U937/III_B cells, both of which continuously produce a large amount of virus without any stimuli (data not shown). As shown in Figure 3A, JTK-101 efficiently suppressed HIV-1 production in MOLT-4/III_B cells even at very low concentrations, yet higher concentrations are required to completely block viral production in MOLT-4/III_B cells than in OM-10.1 cells. Again, K-37 was less active than JTK-101. The EC_{50}s of JTK-101 and K-37 in MOLT-4/III_B cells were 0.0057 and 0.074 μM, respectively (Table 1). Interestingly, little, if any, suppression of HIV-1 production by JTK-101 was observed in U937/III_B cells even at high concentrations (Figure 3B). In contrast, K-37 had similar inhibitory effect on HIV-1 production in MOLT-4/III_B and U937/III_B cells (Figure 3C and 3D). The NRTI 3TC was totally inactive in these chronically infected cells, such as OM-10.1 and MOLT-4/III_B (Table 1).

Antiviral activity in acutely infected cells

In the next experiment, JTK-101 was examined for its inhibition of HIV-1 (III_B strain) replication in acutely infected CEM cells and PBMCs. Although JTK-101 could suppress p24 antigen production in culture supernatants at non-toxic concentrations, the compound was found to be less inhibitory to HIV-1 replication in acutely infected cells than in chronically infected cells (Tables 1 and 2). The EC_{50} and CC_{50} of JTK-101 for HIV-1_{IIIB} in CEM cells were 0.031 and 1.0 μM, respectively, and its EC_{50} and CC_{50} in PBMCs were 0.39 and 1.2 μM, respectively (Table 2). Furthermore, JTK-101 also showed similar antiviral activity against the dual-tropic isolate HE and the R5 clinical isolate CTV in acutely infected MOLT-4 cells and PBMCs, respectively (data not shown). Unlike JTK-101, K-37 appeared to be equally inhibitory to HIV-1 replication in acutely and chronically infected cells (Tables 1 and 2). AZT was a highly potent inhibitor of HIV-1 replication in acutely infected CEM cells.

Inhibitory effect on HIV-1 transcription

As JTK-101 was selected through screening in an HIV-1 LTR-driven reporter gene expression system and showed potent anti-HIV-1 activity in chronically infected cells, the compound was assumed to be an HIV-1 transcription inhibitor. Therefore, quantitative RT-PCR analysis was conducted to determine whether JTK-101 could prevent HIV-1 mRNA synthesis in TNF-α-stimulated OM-10.1 cells. As shown in Figure 4, JTK-101 selectively suppressed TNF-α-induced HIV-1 mRNA synthesis in a dose-dependent fashion. Even at a concentration of 1 nM, the compound could prevent HIV-1 mRNA synthesis by 60% in the cells. By contrast, it did not affect glyceraldehydes-3-phosphate dehydrogenase (GAPDH) mRNA synthesis at concentrations up to 100 nM, indicating that JTK-101 selectively inhibits HIV-1 growth at the transcriptional level.

Inhibitory effects on TNF-α- and Tat-induced transactivation

To elucidate whether JTK-101 primarily inhibits Tat or the cellular transcriptional factor NF-κB, transfection experiments with a Tat expression plasmid into W-3 and KM-3 cells were conducted. Transfection with the Tat expression plasmid induced an increase of SEAP production in both W-3 and KM-3 cells. In contrast, treatment with TNF-α

Figure 3. Inhibitory effects of JTK-101 and K-37 on HIV-1 replication in MOLT-4/III_B and U937/III_B cells

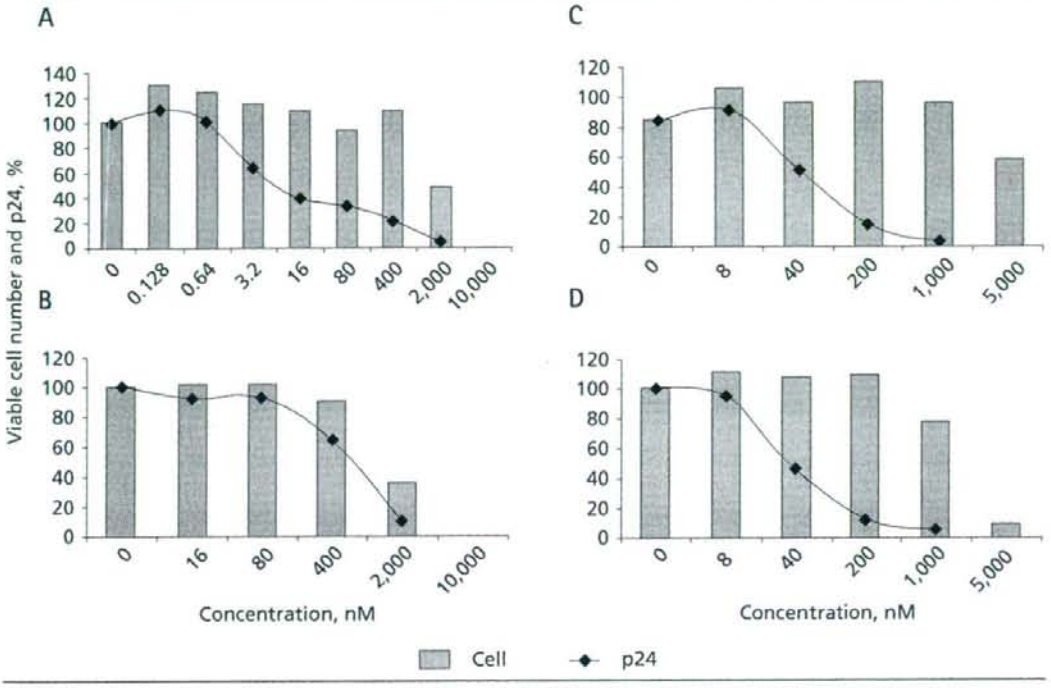

(A) Inhibitory effects of JTK-101 in MOLT-4/III_B cells. **(B)** Inhibitory effects of JTK-101 in U937/III_B cells. **(C)** Inhibitory effects of K-37 in MOLT-4/III_B cells. **(D)** Inhibitory effects of K-37 in U937/III_B cells. MOLT-4/III_B and U937/III_B cells were cultured in the absence or presence of the test compounds without any stimuli. After 3 days of incubation, the p24 antigen levels of culture supernatants (lines) were measured by antigen ELISA. At the same time, the number of viable cells was determined by the 3-(4,5-dimethylthiazol-2-yl)-2,5-diphenyltetrazolium bromide (MTT) method (columns). The experiments were repeated three times and representative results are shown.

Table 2. Inhibitory effects of JTK-101 and other selected compounds on HIV-1 replication in acutely infected cells*

Compound	Cells	EC_{50}†, μM	CC_{50}‡, μM	SI§
JTK101	CEM	0.031 ±0.007	1.0 ±0.5	32
	PBMC	0.39 ±0.25	1.2 ±0.9	3.1
K-37	CEM	0.11 ±0.07	1.8 ±0.6	16
	PBMC	0.095 ±0.074	3.2 ±0.5	34
AZT	CEM	0.0026 ±0.0005	>1	>385

*All data represent means ±SD for three separate experiments. †Concentration required for 50% inhibition of p24 antigen production in culture supernatants. ‡Concentration required for 50% inhibition of cell proliferation and viability. §Selectivity index (ratio of CC_{50} to EC_{50}).

(10 ng/ml) induced an increase of SEAP production in W-3 cells, but not KM-3 cells, because two NF-κB binding sites of the HIV-1 LTR were mutated in KM-3 cells (Baba *et al.*, 1999). In both W-3 and KM-3 cells, JTK-101 could reduce the Tat-induced SEAP production in a dose-dependent fashion (Figure 5A). Interestingly, JTK-101 reduced the Tat-induced SEAP production more efficiently in KM-3 cells than in W-3 cells – its IC_{50} values in W-3 and KM-3 cells were 110 and 4.5 nM, respectively. K-37 inhibited Tat-induced SEAP production less than JTK-101. However, there was no substantial difference between K-37's activity in W-3 and KM-3 cells. The IC_{50} of K-37 in W-3 and KM-3 cells were 318 and 236 nM, respectively (Figure 5B). Furthermore, JTK-101 could reduce the TNF-α-induced SEAP production in W-3 cells with an IC_{50} of 229 nM, whereas K-37 had no effect on the

Figure 4. Inhibitory effects of JTK-101 on HIV-1 mRNA synthesis in OM-10.1 cells

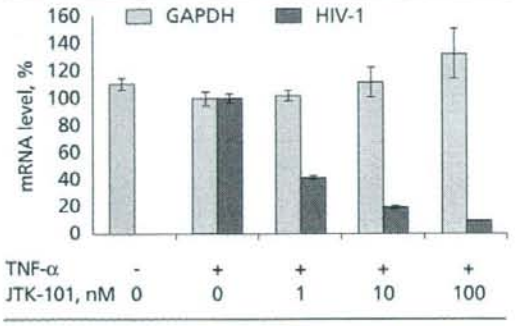

The cells were incubated with the compound for 2 h, stimulated (+) with tumour necrosis factor (TNF)-α (1 ng/ml), and further incubated. After 24 h incubation, total RNA was extracted from the cells, and quantitative RT-PCR for HIV-1 mRNA was performed. The cytotoxic effects of the test compounds on host cellular mRNA synthesis were determined by quantitative RT-PCR for glyceraldehydes-3-phosphate dehydrogenase (GAPDH) mRNA. Representative results for two independent experiments are shown.

TNF-α-induced SEAP production (Figure 5C and 5D). In both cell systems, the compounds did not affect basal SEAP production (data not shown). These results suggest that JTK-101 is capable of inhibiting both Tat- and NF-κB-triggered gene expressions. However, the compound seems to predominantly interfere with a Tat-associated mechanism rather than a NF-κB-associated one. Both JTK-101 and K-37 were found to efficiently inhibit PMA- and TSA-induced HIV-1 production in OM-10.1 cells (data not shown).

CDK9/cyclin T1 level and JTK-101 activity

As the expression of CDK9 and cyclin T1 affect the transactivation by Tat, the protein levels of CDK9 and cyclin T1 were evaluated in several chronically infected cells. As shown in Figure 6, CDK9 and cyclin T1 were highly expressed in the T-lymphoblastoid cell lines CEM and MOLT-4. However, only low levels of the molecules were detected in the promonocytic cell line U937. Chronic infection of MOLT-4 and U937 cells with HIV-1 did not significantly alter the expression of CDK9 and cyclin T1. Furthermore, like MOLT-4/III_B cells, OM-10.1 cells displayed high level expression of CDK9 and cyclin T1. These results suggest that the poor activity of JTK-101 against HIV-1 production in U937/III_B is partly attributed to the low level expression of CDK9 and cyclin T1.

It was reported that the downregulation of cyclin T1 expression at a late stage of M/Ms differentiation contributed to low or absent Tat transactivation function at this stage (Liou *et al.*, 2002). Therefore, the level of CDK9 and cyclin T1 expression and the anti-HIV-1 activity of JTK-101 were examined in differentiated and chronically infected M/Ms. As expected, the expression of cyclin T1 was an undetectable level in both uninfected and chronically infected M/Ms after 17 days of cultivation (Figure 7A). CDK9 was also undetectable, although activated PBMCs obtained from the same donor displayed a high level of cyclin T1 and CDK9 expression. Furthermore, JTK-101 did not inhibit HIV-1 production in chronically infected M/Ms (Figure 7B), whereas K-37 did inhibit HIV-1 production in a dose-dependent fashion (data not shown). These results suggest that the interaction of JTK-101 with either cyclin T1 or CDK9, or both, is needed to exert its anti-HIV-1 activity.

Discussion

The presence of reservoir cells that contain latent viruses results in the prodcution of infectious particles upon cellular activation, which leads to a rebound of the viral load after interruption of HAART (Pierson *et al.*, 2000). The persistence of these virus reservoirs, despite prolonged HAART treatments, represents a major obstacle to the eradication of HIV-1 in infected patients (Finzi *et al.*, 1997; Wong *et al.*, 1997). Therefore, therapeutic targets for HIV-1 replication at the level of transcriptional activation hold great potential for further attempts at clearing viral latency. In this study, we have identified JTK-101, a novel naphthalene derivative, as a potent and selective transcription inhibitor of HIV-1 in latently and chronically infected cells. JTK-101 did not prevent proviral DNA synthesis (data not shown), suggesting that viral entry, uncoating, reverse transcription and integration are not the target of this compound. Furthermore, the inhibition of HIV-1 transcription by JTK-101 is potent and selective. Quantitative RT-PCR analysis revealed that JTK-101 almost completely inhibited HIV-1 mRNA synthesis without altering the level of GAPDH mRNA in TNF-α-treated OM-10.1 cells at a concentration of 100 nM (Figure 4).

K-37, an anti-HIV-1 fluoroquinoline derivative, also displayed selective inhibition of HIV-1 replication in acutely and chronically infected cells (Tables 1 and 2). However, its antiviral activity was weaker than that of JTK-101. K-37 was capable of inhibiting RNA-dependent transactivation mediated by Tat, but did not inhibit DNA-dependent transactivation mediated by NF-κB (Baba *et al.*, 1998; Okamoto *et al.*, 2000). Furthermore, K-37 did not inhibit but stimulated the NF-κB-mediated transactivation at the highest concentration tested (1,000 nM), yet the mechanism was still unknown (Figure 5D). Unlike K-37, JTK-101 could inhibit not only Tat but also NF-κB-mediated transactivation of the HIV-1 LTR (Figure 5). Although JTK-101 was highly inhibitory to Tat-mediated transactivation, a much higher concentration

Figure 5. Inhibitory effects of JTK-101 and K-37 on HIV-1 Tat-induced or TNF-α-induced transactivation in W-3 and KM-3 cells

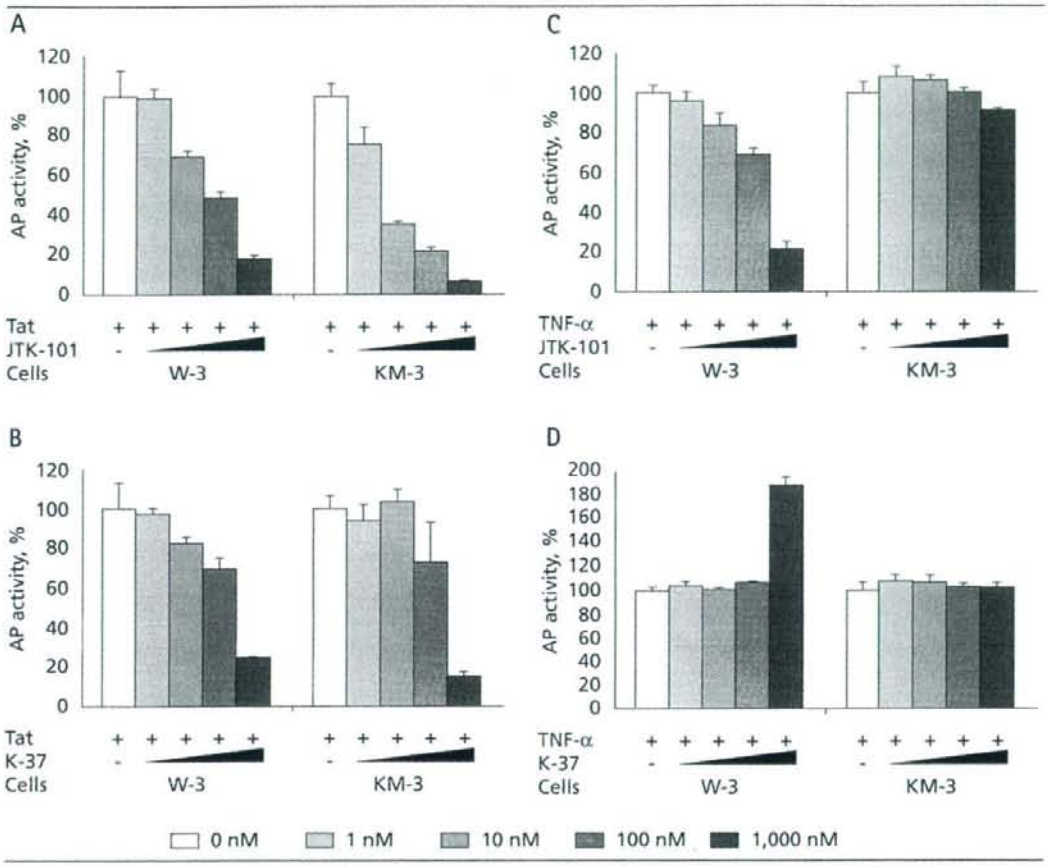

For HIV-1 Tat-induced transactivation **(A and B)**, W-3 and KM-3 cells were transfected with the Tat expression plasmid (1 μg). For tumour necrosis factor (TNF)-α-induced transactivation **(C and D)**, W-3 and KM-3 cells were treated with or without TNF-α (10 ng/ml). The cells were cultured in the presence of various concentrations of the compounds. After 2 days of incubation, the culture supernatants were collected and examined for their secreted alkaline phosphatase (SEAP) levels. At the same time, the number of viable cells was determined by the 3-(4,5-dimethylthiazol-2-yl)-2,5-diphenyltetrazolium bromide (MTT) methods. Transfection with the Tat expression plasmid induced 8.8- and 6.3-fold increase of SEAP production in W-3 and KM-3 cells, respectively. While TNF-α stimulation induced 3.5- and 0.9-fold increases of SEAP production in W-3 and KM-3 cells, respectively. Effects of JTK-101 **(A and C)** and K-37 **(B and D)** on TNF-α- or HIV-1 Tat-induced transactivation were expressed as percent inhibition of SEAP activity. All experiments were carried out in duplicate and expressed as means (ranges). Representative results for two independent experiments are shown.

was required to inhibit NF-κB-mediated transactivation. Thus, it is assumed that JTK-101 exerts its potent anti-HIV-1 activity primarily through the inhibition of Tat function rather than NF-κB. Furthermore, JTK-101 was still active against HIV-1 replication in OM-10.1 cells, even when added to culture medium 24 h after stimulation with TNF-α (data not shown). The compound showed a similar inhibitory effect on TSA-induced HIV-1 production in OM-10.1 cells (data not shown), further suggesting that NF-κB was not a major target. Although the cellular transcription factor NF-κB plays an important role in triggering HIV-1 gene expression, the activation of NF-κB leads to rapid production of Tat, which may be necessary to maintain continuous HIV-1 gene expression in latently infected cells. Therefore, as well as NF-κB inhibitors, a Tat inhibitor could be effective in restricting the recovery of latent virus from resting T cells *in vivo*. Stevens *et al.* (2007) recently reported that N-aminoimidazole derivatives interfered with viral replication at a post-integrational level by inhibiting HIV-1 mRNA transcription. However,

Figure 6. Western blot analysis for CDK9 and cyclin T1 expression in various cell lines

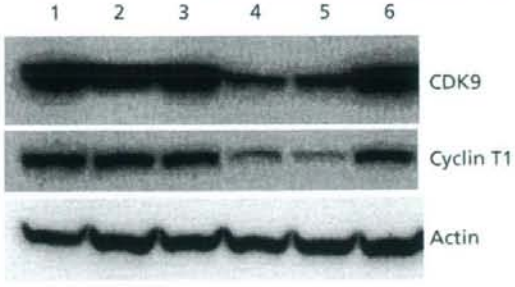

Whole cell-lysates were fractionated by 10% sodium dodecyl sulphate-polyacrylamide gels, and western blot analysis was performed with anti-CDK9, anti-cyclin T1 or anti-actin polyclonal antibodies. The analysed samples were CEM cells (lane 1), MOLT-4 cells (lane 2), MOLT-4/III_B cells (lane 3), U937 cells (lane 4), U937/III_B cells (lane 5) and OM-10.1 cells (lane 6).

Figure 7. CDK9 and cyclin T1 expression in chronically infected M/Ms and anti-HIV-1 activity of JTK-101

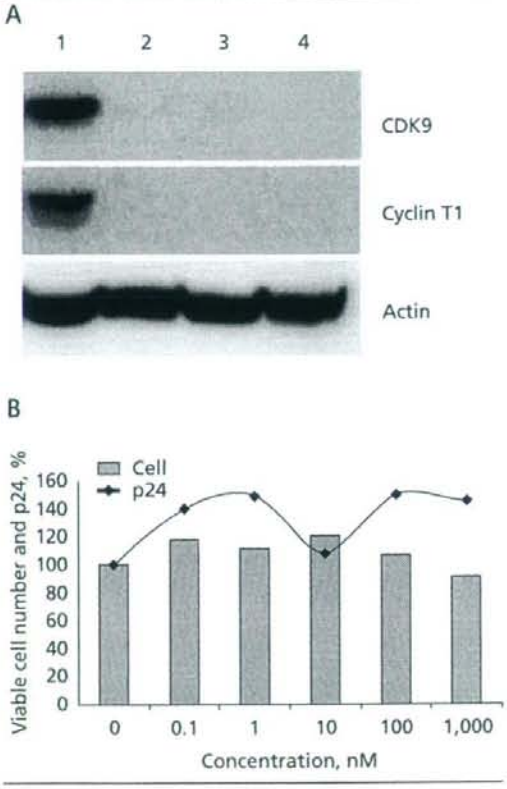

(A) The isolated monocytes/macrophages (M/Ms) were kept uninfected (lane 2) or infected with HIV-1_{BaL} on day 2 (lane 3) or day 7 (lane 4). After 24 h incubation, the cells were washed and further incubated. On day 17, the cells were harvested for cell extracts preparation. Western blot analysis was performed, as described in Figure 6. The culture supernatants were also collected on day 17 for p24 antigen detection. Their p24 levels of infected M/Ms on days 2 and 7 were 221.5 and 27.3 ng/ml, respectively. As a control, peripheral blood mononuclear cells (PBMCs) from same donors stimulated with phytohaemagglutinin (PHA) for 3 days were also examined (lane 1). **(B)** Inhibitory effects of JTK-101 on HIV-1 replication in chronically infected M/Ms. The isolated M/Ms were cultured for 7 days and infected with HIV-1_{BaL}. After 24 h of incubation, the cells were washed and cultured for further 9 days. After extensive washing, chronically infected M/Ms were cultured in the presence of various concentrations of JTK-101. After 4 days of incubation, the p24 antigen levels of culture supernatants (lines) were measured by ELISA. At the same time, the number of viable cell was determined by the 3-(4,5-dimethylthiazol-2-yl)-2,5-diphenyltetrazolium bromide (MTT) method (columns). The experiments were repeated four times with PBMCs obtained from different donors; representative results are shown.

unlike JTK-101, these compounds enhanced NF-κB binding at the HIV-1 promoter. Furthermore, they suppressed viral transcription via potent inhibitory effects on the recruitment of Tat to the HIV-1 promoter and on the transcriptional processivity of RNA polymerase II during the viral transcription process (Stevens *et al.*, 2007).

In spite of robust inhibition of HIV-1 replication in the chronically infected cells OM-10.1 and MOLT-4/III_B, JTK-101 did not produce a significant inhibitory effect in U937/III_B cells and primary M/Ms. It showed less inhibitory to HIV-1 replication in acutely infected cells, especially in acutely infected PBMCs, than in chronically infected cells This difference in anti-HIV-1 activity between acute and chronic stages of infection could be attributed to a distinct role of Tat in the infection stage or to the possibility that the compound interacts with known or unknown cellular factors involved in Tat-mediated transactivation.

Several lines of evidence have suggested that Tat function is largely dependent upon the interaction with the cellular transcription factor TAK/P-TEFb, a complex containing cyclin T1 and CDK9 (Herrmann & Rice, 1995; Mancebo *et al.*, 1997). In fact, several CDK inhibitors were found to potently suppress Tat functions and inhibited HIV-1 replication in cell cultures (Heredia *et al.*, 2005; Wang *et al.*, 2001). Our preliminary experiments demonstrated that JTK-101 could inhibit CDK9 with an IC_{50} of 0.3 μM, whereas it did not show any inhibition of CDK7 and casein kinase II (data not shown). Although direct interaction between JTK-101 and CDK9 has not been demonstrated, its activity was totally dependent on the expression of CDK9 and cyclin T1 in infected cells. The expression of TAK/P-TEFb, especially cyclin T1, was regulated during differentiation from monocytes to macrophages. PMA, vitamin D_3 and other agents cause the human myelomonocytic cell line HL-60 and the promonocytic cell line U937 to differentiate into terminal cells exhibiting macrophage characteristics, accompanied by a dramatic increase in their cyclin T1 levels (Herrmann *et al.*,

1998). Furthermore, the cyclin T1 level in freshly isolated monocytes increases during the first 2–3 days in the differentiation process then starts decreasing to a very low level after 10 days (Liou *et al.*, 2002). As cyclin T1 is essential for the Tat function, it is possible that cyclin T1 regulates HIV-1 replication in certain types of cells. In fact, it has been reported that the level of cyclin T1 expression regulates Tat transactivation of the HIV-1 LTR in promonocytic cells and primary M/Ms (Herrmann *et al.*, 1998; Liou *et al.*, 2002). The transactivation activity of Tat was always weak or absent when cyclin T1 expression was very low. In such cells as U937 and primary M/Ms, JTK-101 may not be able to intervene between Tat and cyclin T1/CDK9 and exert its anti-HIV-1 activity.

Another interesting finding is that the inhibitory effect of JTK-101 on Tat-mediated transactivation was still affected by the function of NF-κB. JTK-101 was more efficient in suppressing Tat-mediated transactivation when the functional NF-κB binding sites were removed from the HIV-1 LTR (Figure 5). A previous study showed that Tat-mediated transactivation of the HIV-1 LTR was strictly dependent on the HIV-1 enhancer, especially NF-κB, in human blood $CD4^+$ T-lymphocytes (Alcami *et al.*, 1995). NF-κB-independent Tat transactivation could occur in transformed lymphoblastoid T-cell lines, but not in normal T lymphocytes (Alcami *et al.*, 1995). Thus, the absolute dependence of Tat function on κB responsive elements in T lymphocytes might bring about the much reduced anti-HIV-1 activity of JTK-101 observed in acutely infected PBMCs as compared with acutely infected CEM cells. Furthermore, Tat upregulates cytokine gene expression via a TAR-independent pathway and induces the production of proinflammatory cytokines, such as TNF-α and interleukin 1β, which activate NF-κB signal transduction pathways (Biswas *et al.*, 1995).

In conclusion, the novel naphthalene derivative JTK-101 is a potent and selective inhibitor of HIV-1 replication in cell cultures. Although its precise target molecule remains to be elucidated, the compound suppresses HIV-1 gene expression through the inhibition of known or unknown Tat cofactors, presumably CDK9/cyclin T1.

Acknowledgements

This work was supported in part by a research grant from the Ministry of Health Labor and Welfare, Japan.

References

Alcami J, Lain de Lera T, Folgueira L, Pedraza MA, Jacque JM, Bachelerie F, Noriega AR, Hay RT, Harrich D, Gaynor RB, Virelizier JL & Arenzana-Seisdedos F (1995). Absolute dependence on kappa B responsive elements for initiation and Tat-mediated amplification of HIV transcription in blood CD4 T lymphocytes. *The EMBO Journal* **14**:1552–1560.

Baba M, Okamoto M, Kawamura M, Makino M, Higashida T, Takashi T, Kimura Y, Ikeuchi T, Tetsuka T & Okamoto T (1998). Inhibition of human immunodeficiency virus type 1 replication and cytokine production by fluoroquinoline derivatives. *Molecular Pharmacology* **53**:1097–1103.

Baba M, Okamoto M & Takeuchi H (1999). Inhibition of human immunodeficiency virus type 1 replication in acutely and chronically infected cells by EM2487, a novel substance produced by a *Streptomyces* species. *Antimicrobial Agents & Chemotherapy* **43**:2350–2355.

Biswas DK, Salas TR, Wang F, Ahlers CM, Dezube BJ & Pardee AB (1995). A Tat-induced auto-up-regulatory loop for superactivation of the human immunodeficiency virus type 1 promoter. *Journal of Virology* **69**:7437–7444.

Butera ST, Perez VL, Wu BY, Nabel GJ & Folks TM (1991). Oscillation of the human immunodeficiency virus surface receptor is regulated by the state of viral activation in a $CD4^+$ cell model of chronic infection. *Journal of Virology* **65**:4645–4653.

Cullen BR (1991). Regulation of human immunodeficiency virus replication. *Annual Review of Microbiology* **45**:219–250.

Finzi D, Hermankova M, Pierson T, Carruth LM, Buck C, Chaisson RE, Quinn TC, Chadwick K, Margolick J, Brookmeyer R, Gallant J, Markowitz M, Ho DD, Richman DD & Siliciano RF (1997). Identification of a reservoir for HIV-1 in patients on highly active antiretroviral therapy. *Science* **278**:1295–1300.

Heredia A, Davis C, Bamba D, Le N, Gwarzo MY, Sadowska M, Gallo RC & Redfield RR (2005). Indirubin-3′-monoxime, a derivative of a Chinese antileukemia medicine, inhibits P-TEFb function and HIV-1 replication. *AIDS* **19**:2087–2095.

Herrmann CH & Rice AP (1995). Lentivirus Tat proteins specifically associated with a cellular protein kinase, TAK, that hyperphosphorylates the carboxyl-terminal domain of the large subunit of RNA polymerase II: candidate for a Tat cofactor. *Journal of Virology* **69**:1612–1620.

Herrmann CH, Carroll RG, Wei P, Jones KA & Rice AP (1998). Tat-associated kinase, TAK, activity is regulated by distinct mechanisms in peripheral blood lymphocytes and promonocytic cell lines. *Journal of Virology* **72**:9881–9888.

Jones KA & Peterlin BM (1994). Control of RNA initiation and elongation at the HIV-1 promoter. *Annual Review of Biochemistry* **63**:717–743.

Liou LY, Herrmann CH & Rice AP (2002). Transient induction of cyclin T1 during human macrophage differentiation regulates human immunodeficiency virus type 1 Tat transactivation function. *Journal of Virology* **76**:10579–10587.

Mancebo HS, Lee G, Flygare J, Tomassini J, Luu P, Zhu Y, Peng J, Blau C, Hazuda D, Price D & Flores O (1997). P-TEFb kinase is required for HIV Tat transcriptional activation *in vivo* and *in vitro*. *Genes & Development* **11**:2633–2644.

Nobel G & Baltimore D (1987). An inducible transcription factor activates expression of human immunodeficiency virus in T cells. *Nature* **326**:711–713.

Okamoto H, Cujec TP, Okamoto M, Peterlin BM, Baba M & Okamoto T (2002). Inhibition of the RNA-dependent transactivation and replication of human immunodeficiency virus type 1 by a fluoroquinoline derivative K-37. *Virology* **272**:402–408.

Okamoto T (1995). Regulatory proteins of human immunodeficiency virus and therapy, in Anti-AIDS drug development: challenges, strategies and prospects. In *Anti-AIDS drug development: challenges, strategies and prospects*. Edited by P Mohan and M Baba. Switzerland: Harwood Academic Publishers, pp.117–127.

Parolin C, Gatto B, Del Vecchio C, Pecere T, Tramontano E, Cecchetti V, Fravolini A, Masiero S, Palumbo M & Palu G (2003). New anti-human immunodeficiency virus type 1 6-aminoquinolones: mechanism of action. *Antimicrobial Agents & Chemotherapy* **47**:889–896.

Pauwels R, Balzarini J, Baba M, Snoeck R, Schols D, Herdewijn P, Desmyter J & De Clercq E (1988). Rapid and automated tetrazolium based colorimetric assay for detection of anti-HIV compounds. *Journal of Virological Methods* **20**:309–312.

Peng J, Zhu Y, Milton JT & Price DH (1998). Identification of multiple cyclin subunits of human P-TEFb. *Genes & Development* **12**:755–762.

Perno CF, Yarchoan R, Cooney DA, Hartman NR, Gartner S, Popovic M, Hao Z, Gerrard TL, Wilson YA, Johns DG & Broder S (1988). Inhibition of human immunodeficiency virus (HIV-1/HTLV-IIIBa-L) replication in fresh and human peripheral blood monocyte/macrophages by azidothymidine and related 2′,3′-dideoxynucleosides. *The Journal of Experimental Medicine* **168**:1111–1125.

Peterlin BM & Trono D (2003). Hide, shield and strike back: how human immunodeficiency virus-infected cells avoid immune eradication. *Nature Reviews Immunology* **3**:97–107.

Pierson T, McArthur J & Siliciano RF (2000). Reservoirs for HIV-1: mechanisms for viral persistence in the presence of antiviral immune responses and antiretroviral therapy. *Annual Review of Immunology* **18**:665–708.

Pomerantz RJ & Horn DL (2003). Twenty years of therapy for HIV-1 infection. *Nature Medicine* **9**:867–873.

Price DH (2000). P-TEFb, a cyclin-dependent kinase controlling elongation by RNA polymerase II. *Molecular & Cellular Biology* **20**:2629–2634.

Richter S, Parolin C, Gatto B, Del Vecchio C, Brocca-Cofano E, Fravolini A, Palu G & Palumbo M (2004). Inhibition of human immunodeficiency virus type 1 Tat-trans-activation-responsive region interaction by an antiviral quinoline derivative. *Antimicrobial Agents & Chemotherapy* **48**:1895–1899.

Roulston A, Lin R, Beauparlant P, Wainberg MA & Hiscott J (1995). Regulation of human immunodeficiency virus type 1 and cytokine gene expression in myeloid cells by NF-κB/Rel transcription factors. *Microbiological Reviews* **59**:481–505.

Stevens M, Balzarini J, Lagoja IM, Noppen B, François K, Van Aerschot A, Herdewijn P, De Clercq E & Pannecouque C (2007). Inhibition of human immunodeficiency virus type 1 transcription by N-aminoimidazole derivatives. *Virology* **356**:220–237.

Wang X, Miyake H, Okamoto M, Saito M, Fujisawa J, Tanaka Y, Izumo S & Baba M (2002). Inhibition of the Tax-dependent human T-lymphotropic virus type I replication in persistently infected cells by the fluoroquinolone derivative K-37. *Molecular Pharmacology* **61**:1359–1365.

Wang D, de la Fuente C, Deng L, Wang L, Zilberman I, Eadie C, Healey M, Stein D, Denny T, Harrison LE, Meijer L & Kashanchi F (2001). Inhibition of human immunodeficiency virus type 1 transcription by chemical cyclin-dependent kinase inhibitors. *Journal of Virology* **75**:7266–7279.

Wei P, Garber ME, Fang SM, Fisher WH & Jones KA (1998). A novel CDK9-associated C-type cyclin interacts directly with HIV-1 Tat and mediates its high-affinity, loop-specific binding to TAR RNA. *Cell* **92**:451–462.

Wong JK, Hezareh M, Gunthard HF, Havlir DV, Ignacio CC, Spina CA & Richman DD (1997). Recovery of replication-competent HIV despite prolonged suppression of plasma viremia. *Science* **278**:1291–1295.

Yeni PG, Hammer SM, Hirsch MS, Saag MS, Schechter M, Carpenter CC, Fischl MA, Gatell JM, Gazzard BG, Jacobsen DM, Katzenstein DA, Montaner JS, Richman DD, Schooley RT, Thompson MA, Vella S & Volberding PA (2004). Treatment for adult HIV infection: 2004 recommendations of the International AIDS Society-USA Panel. *The Journal of the American Medical Association* **292**:251–265.

Received 5 April 2007, accepted 15 May 2007

THE JOURNAL OF BIOLOGICAL CHEMISTRY VOL. 282, NO. 39, pp. 28709–28720, September 28, 2007
Printed in the U.S.A.

Potent Inhibition of HIV-1 Replication by Novel Non-peptidyl Small Molecule Inhibitors of Protease Dimerization*

Received for publication, May 14, 2007, and in revised form, June 25, 2007 Published, JBC Papers in Press, July 17, 2007, DOI 10.1074/jbc.M703938200

Yasuhiro Koh[‡§], Shintaro Matsumi[‡§], Debananda Das[¶], Masayuki Amano[‡§], David A. Davis[‖], Jianfeng Li[**], Sofiya Leschenko[**], Abigail Baldridge[**], Tatsuo Shioda[‡‡], Robert Yarchoan[‖], Arun K. Ghosh[**], and Hiroaki Mitsuya[‡§¶1]

From the [‡]Department of Hematology and [§]Department of Infectious Diseases, Kumamoto University Graduate School of Medical and Pharmaceutical Sciences, 1-1-1 Honjo, Kumamoto 860-8556, Japan, the [¶]Experimental Retrovirology Section and [‖]Retroviral Disease Section, HIV and AIDS Malignancy Branch, NCI, National Institutes of Health, Bethesda, Maryland 20892, the [**]Departments of Chemistry and Medicinal Chemistry, Purdue University, West Lafayette, Indiana 47907, and the [‡‡]Department of Viral Infections, Research Institute for Microbial Diseases, Osaka University, Osaka 565-0871, Japan

Dimerization of HIV-1 protease subunits is essential for its proteolytic activity, which plays a critical role in HIV-1 replication. Hence, the inhibition of protease dimerization represents a unique target for potential intervention of HIV-1. We developed an intermolecular fluorescence resonance energy transfer-based HIV-1-expression assay employing cyan and yellow fluorescent protein-tagged protease monomers. Using this assay, we identified non-peptidyl small molecule inhibitors of protease dimerization. These inhibitors, including darunavir and two experimental protease inhibitors, blocked protease dimerization at concentrations of as low as 0.01 μM and blocked HIV-1 replication with IC_{50} values of 0.0002–0.48 μM. These agents also inhibited the proteolytic activity of mature protease. Other approved anti-HIV-1 agents examined except tipranavir, a CCR5 inhibitor, and soluble CD4 failed to block the dimerization event. Once protease monomers dimerize to become mature protease, mature protease is not dissociated by this dimerization inhibition mechanism, suggesting that these agents block dimerization at the nascent stage of protease maturation. The proteolytic activity of mature protease that managed to undergo dimerization despite the presence of these agents is likely to be inhibited by the same agents acting as conventional protease inhibitors. Such a dual inhibition mechanism should lead to highly potent inhibition of HIV-1.

Highly active antiretroviral therapy has had a major impact on the AIDS epidemic in industrially advanced nations. However, eradication of human immunodeficiency virus, type 1 (HIV-1)[2] does not appear to be currently possible, in part due to the viral reservoirs remaining in blood and infected tissues. Moreover, a number of challenges have been encountered, which include various adverse effects, only partial and limited immunologic restorations achieved, and occurrence of various cancers as consequences of survival elongation with highly active antiretroviral therapy (1). Moreover, such limitations of highly active antiretroviral therapy are exacerbated by the development of drug-resistant HIV-1 variants (2). Thus, the identification of new classes of antiretroviral drugs that have one or more unique mechanisms of action and produce no or minimal adverse effects remains an important therapeutic objective.

Dimerization of HIV-1 protease subunits is an essential process for the acquisition of proteolytic activity of HIV-1 protease, which plays a critical role in the maturation and replication of the virus (3, 4). Thus inhibition of protease dimerization by chemical reagents is likely to abolish proteolytic activity and inhibit HIV-1 replication. However, for possible development of HIV-1 protease dimerization inhibitors, better understanding of the nature and dynamics of protease dimerization is crucial. The monomer subunits are connected by polar and non-polar interactions to form the dimer. Hydrophobicity of Leu-89, Leu-90, and Ile-93 and several other residues have been considered important in the folding of a protease monomer as well as in dimer stabilization (5, 6). For a systematic analysis of the conserved network of hydrogen bonds, termed "fireman's grip," Strisovsky *et al.* (7) have mutated the active site Thr-26 to a Ser, Cys, or Ala and have shown that T26A substitution reduced protease dimer stability, thus virtually nullifying the proteolytic activity of protease. Indeed, in our present study, T26A substitution effectively disrupted protease dimerization (see below), corroborating the results by Strisovsky *et al.* The flexibility of monomeric and dimeric HIV-1 protease and the feasibility of a stable protease monomer have also been studied

* This work was supported by the Intramural Research Program of Center for Cancer Research, NCI, National Institutes of Health (NIH), by a Grant-in-aid for Scientific Research (Priority Areas) from the Ministry of Education, Culture, Sports, Science, and Technology of Japan (Monbu-Kagakusho), a Grant for Promotion of AIDS Research from the Ministry of Health, Welfare, and Labor of Japan (Kosei-Rohdosho), by the Cooperative Research Project on Clinical and Epidemiological Studies of Emerging and Re-emerging Infectious Diseases (Renkei Jigyo: Grant 78, Kumamoto University) of Monbu-Kagakusho, by the Japan Health Sciences Foundation (International Research Grant SA14801 to H. M. and A. K. G.), and by NIH Grant GM 53386 (to A. K. G.). The costs of publication of this article were defrayed in part by the payment of page charges. This article must therefore be hereby marked "*advertisement*" in accordance with 18 U.S.C. Section 1734 solely to indicate this fact.

[1] To whom correspondence should be addressed: Tel.: 81-96-373-5156; Fax: 81-96-363-5265; E-mail: hmitsuya@helix.nih.gov.

[2] The abbreviations used are: HIV-1, human immunodeficiency virus, type 1; FRET, fluorescence resonance energy transfer; CFP, cyan fluorescent protein; YFP, yellow fluorescent protein; BCV, brecanavir; DRV, darunavir; CHX, cycloheximide; PI, protease inhibitor; bis-THF, bistetrahydrofuranylurethane; TPV, tipranavir; Fluc, firefly luminescence; Rluc, *Renilla* luminescence; RT, reverse transcriptase; PR, protease.

by computational simulation (8, 9). There are four anti-parallel β-sheets involving the N and C termini of both monomer subunits and they contribute close to 75% of the dimerization energy (10), explaining at least in part why DRV failed to dissociate mature protease dimer (see below). The termini interface has been explored as a dimerization inhibition target by several groups (11–13). We have also recently reported that certain peptides containing the dimer interface sequences amino acids 1–5 and amino acids 95–99 blocked HIV-1 infectivity and replication (14). However, to the best of our knowledge, no evidence of direct dimerization inhibition by such compounds has been yet documented.

In the present study, we developed an intermolecular fluorescence resonance energy transfer (FRET)-based HIV-1-expression assay that employed cyan and yellow fluorescent protein-tagged HIV-1 protease monomers. Using this assay, we identified a group of non-peptidyl small molecule inhibitors of HIV-1 protease dimerization. These inhibitors, including the recently approved protease inhibitor (PI) darunavir (DRV) as well as two experimental protease inhibitors (PIs), blocked protease dimerization at concentrations of as low as 0.01 μM and blocked HIV-1 replication *in vitro* with IC_{50} values of 0.0002–0.48 μM. These agents also inhibited the proteolytic activity of mature HIV-1 protease. Another PI, tipranavir (TPV), active against HIV-1 variants resistant to multiple PIs, also blocked protease dimerization, although all other existing FDA-approved anti-HIV-1 drugs examined in the present study failed to block the dimerization. The present report represents the first demonstration that non-peptidic small molecule agents can disrupt protease dimerization.

EXPERIMENTAL PROCEDURES

Generation of FRET-based HIV-1 Expression System—Cyan fluorescent protein (CFP)- and yellow fluorescent protein (YFP)-tagged HIV-1 protease constructs were generated using BD Creator™ DNA cloning kits (BD Biosciences, San Jose, CA). First, XhoI/HindIII fragments from pCR-XL-TOPO vector containing the HIV-1 protease-encoding gene excised from pHIV-1_{NL4-3} was inserted into the pDNR-1r (donor vector) that had been digested with XhoI and HindIII. In the transfer of the protease gene from the donor vector into pLP-CFP/YFP-C1 (acceptor vector), the Cre-loxP site-specific recombination method was used according to manufacturer's instructions. Using Cre-recombinase with the lox P site, the protease gene from pDNR-1r was inserted into pLP-CFP-C1 or pLP-YFP-C1 through Cre-mediated recombination (15), generating a plasmid of CFP-tagged wild type protease (PR_{WT}) and that of YFP-tagged PR_{WT}, with which HIV-1 protease was successfully expressed as a fusion protein with CFP- and YFP-tagged at the C terminus, respectively. Western blot assay using anti-green fluorescent protein-specific rabbit polyclonal antibodies revealed that protease was correctly tagged to CFP or YFP (data not shown).

For the generation of full-length molecular infectious clones containing CFP- or YFP-tagged protease, the PCR-mediated recombination method was used (16). To this end, we amplified an upstream proviral DNA fragment containing ApaI site and HIV-1 protease (excised from pHIV-1_{NL4-3}) with a primer pair: Apa-PRO-F (5′-TTG CAG GGC CCC TAG GAA AAA GG-3′) plus PR-5Ala-R (5′-GGC TGC TGC GGC AGC AAA ATT TAA AGT GCA GCC AAT CT-3′), a middle proviral DNA fragment containing CFP (excised from pCFP-C1) or YFP (excised from pYFP-C1) (Clontech, Mountain View, CA) with a primer pair: CFPYFP-5Ala-F (5′-GCT GCC GCA GCA GCC GTG AGC AAG GGC GAG GAG CTG-3′) plus CFPYFP-FP-R (5′-ACT AAT GGG AAA CTT GTA CAG CTC GTC CAT GCC G-3′), and a downstream proviral DNA fragment containing the 5′-DNA fragment of reverse transcriptase (RT) and SmaI site from pHIV-1_{NLSma} (17), which had been created to have a SmaI site by changing two nucleotides (2590 and 2593) of pHIV-1_{NL4-3} with a primer pair: FRT-F (5′-TTT CCC ATT AGT CCT ATT GAG ACT GTA-3′) plus NL4-3-RT263-R (5′-CCA GAA ATC TTG AGT TCT CTT ATT-3′). A linker consisting of five alanines was inserted between protease and fluorescent protein. The phenylalanine-proline site that HIV-1 protease cleaves was also introduced between the fluorescent protein and RT. Thus obtained three DNA fragments were subsequently joined by using the PMR reaction performed under the standard condition for ExTaq polymerase (Takara Bio Inc., Otsu, Japan) with 10 pmol of Apa-PRO-F (5′-TTG CAG GGC CCC TAG GAA AAA GG-3′) and NL4-3-RT263-R (5′-CCA GAA ATC TTG AGT TCT CTT ATT-3′) and the three DNA fragments (100 ng each) in a 20-μl reaction solution. Thermal cycling was carried out as follows: 94 °C for 3 min, followed by 35 cycles of 94 °C for 50 s, 53 °C for 50 s, and 72 °C for 2 min, and finally by 72 °C for 15 min. The amplified PCR products were cloned into pCR-XL-TOPO vector according to the manufacturer's instructions (Gateway Cloning System, Invitrogen). PCR products were generated with pCR-XL-TOPO vector as templates, followed by digestion by both ApaI and SmaI, and the ApaI-SmaI fragment was introduced into pHIV-1_{NLSma} (17), generating pHIV-PR_{WT}^{CFP} and pHIV-PR_{WT}^{YFP}, respectively.

Analysis of Inter- and Intra-molecule Interactions of Protease Subunits—Analysis of inter- and intra-molecule interactions of protease subunits was conducted by employing the crystal structure of DRV with HIV-1 protease (PDB ID: 2IEN). Hydrogens were added and minimized using the OPLS2005 force field with constraints on heavy atom positions. The calculation was performed using MacroModel 9.1 from Schrödinger, LLC. Hydrogen bonds were assigned when the following distance and angle cut-off was satisfied: 3.0 Å for H-A distance; D-H-A angle >90°; and H-A-B angle >60° where H is the hydrogen, A is the acceptor, D is the donor, and B is a neighbor atom bonded to the acceptor. The representative distance between the termini of two monomers was determined by analyzing the protease-DRV crystal structure (PDB ID: 2IEN). The distance between the α carbons at the N termini and C termini is around 0.5 nm, whereas the distance between the α carbons of the N termini ends of two monomers is around 1.8 nm.

FRET Procedure—COS7 cells plated on EZ view cover-glass bottom culture plate (Iwaki, Tokyo) were transfected with the indicated plasmid constructs using Lipofectamine 2000 (Invitrogen) according to manufacturer's instructions in the presence of various concentrations of each compound, cultured for 72 h, and analyzed under Fluoview FV500 confocal laser scanning microscope (Olympus Optical Corp., Tokyo) at room

temperature. When the effect of each compound was analyzed by FRET, test compounds were added to the culture medium simultaneously with plasmid transfection.

The results of FRET were determined by quenching of CFP (donor) fluorescence and an increase in YFP (acceptor) fluorescence (sensitized emission), because part of the energy of CFP is transferred to YFP instead of being emitted. This phenomenon can be measured by bleaching YFP, which should result in an increase in CFP fluorescence. This technique, also known as acceptor photobleaching, is a well established method of determining the occurrence of FRET (18–21). Dequenching of the donor CFP by selective photobleaching of the acceptor YFP was performed by first obtaining YFP and CFP images at the same focal plane, followed by illuminating for 3 min the same image at a wavelength of 488 nm with a laser power set at the maximum intensity to bleach YFP and re-capturing the same CFP and YFP images. The changes in the CFP and YFP fluorescence intensity in the images of selected regions were examined and quantified using Olympus FV500 Image software system (Olympus Optical Corp.). Background values were obtained from the regions where no cells were present and were subtracted from the values for the cells examined in all calculations. For each chimeric protein, the data were obtained from at least three independent experiments. Digitized image data obtained from the experiment were prepared for presentation using Photoshop 6.0 (Adobe Systems, Mountain View, CA). Ratios of intensities of CFP fluorescence after photobleaching to CFP fluorescence prior to photobleaching ($CFP^{A/B}$ ratios) were determined. It is well established that the $CFP^{A/B}$ ratios of >1.0 indicate that association of CFP- and YFP-tagged proteins occurred, and it was interpreted that the dimerization of protease subunits occurred. When the $CFP^{A/B}$ ratios were <1, it indicated that the association of the two subunits did not occur, and it was interpreted that protease dimerization was inhibited.

Non-peptidyl Small Molecule Compounds—Seven non-peptidyl small molecule compounds were synthesized in a convergent manner by coupling an optically active P2 ligand and an (*R*)-hydroxyethylamino sulfonamide isostere (22). Synthetic methods for TMC126 and DRV have been previously described (22, 23). Detailed synthetic methods for the other four compounds will be described elsewhere. TPV was obtained through the AIDS Research and Reference Reagent Program, Division of AIDS, NIAID, National Institutes of Health.

Dual Luciferase Assay—Dual luciferase assay was established using the CheckMate™ Mammalian Two-Hybrid System (Promega Corp., Madison, WI). Briefly, BamHI/KpnI fragments from pCR-XL-TOPO vector containing the HIV-1 protease (PR_{WT})-encoding gene excised from $pHIV\text{-}1_{NL4\text{-}3}$ was inserted into the pACT vector and pBIND vector that had been digested with BamHI and KpnI, generating pACT-PR_{wt} and pBIND-PR_{wt}, which produced an in-frame fusion of wild-type HIV-1 protease downstream of the VP16 activation domain and GAL4 DNA-binding domain, respectively. COS7 cells were co-transfected with pACT-PR_{wt}, pBIND-PR_{wt}, and pG5*luc* in the absence or presence of 0.1 or 1.0 μM DRV in white 96-well flat bottom plates (Corning, NY), cultured for 48 h, and the intensity of firefly luminescence (Fluc) and *Renilla* luminescence (Rluc) was measured with TR717 microplate luminometer (Applied Biosystems) according to the manufacturer's instructions. DRV was added to the culture medium simultaneously with plasmids to be used. Fluc/Rluc intensity ratios were determined with co-transfection of pACT-PR_{WT}, pBIND-PR_{WT}, and pG5*luc* in the absence of DRV, serving as maximal values. Fluc/Rluc intensity ratios determined with co-transfection of a pACT vector, a pBIND vector, and pG5*luc* served as minimal (background) values. Relative response ratios (RRR) were determined using the following formula: RRR = [(experimental Fluc/Rluc) − (negative control Fluc/Rluc)]/[(positive control Fluc/Rluc) − (negative control Fluc/Rluc)].

Drug Susceptibility Assay—The susceptibility of $HIV\text{-}1_{LAI}$ to various drugs and their cytotoxicity were determined using the 3-(4,5-dimethylthiazol-2-yl)-2,5-diphenyltetrazolium bromide assay as previously described (24). Briefly, MT-2 cells (2×10^4/ml) were exposed to 100 50% tissue culture infectious doses ($TCID_{50}$s) of $HIV\text{-}1_{LAI}$ in the presence or absence of various concentrations of drugs in 96-well microculture plates and cultured at 37 °C for 7 days. After 100 μl of the medium was removed from each well, 3-(4,5-dimetylthiazol-2-yl)-2,5-diphenyltetrazolium bromide solution (10 μl, 7.5 mg/ml in phosphate-buffered saline) was added to each well, followed by incubation at 37 °C for 4 h. After incubation, 100 μl of acidified isopropanol containing 4% (v/v) Triton X-100 was added to each well, to dissolve the formazan crystals, and the optical density was measured in a kinetic microplate reader (V_{max}, Molecular Devices, Sunnyvale, CA). All assays were performed in duplicate or triplicate. In some experiments, MT-2 cells were chosen as target cells in the 3-(4,5-dimethylthiazol-2-yl)-2,5-diphenyltetrazolium bromide assay, because these cells undergo greater HIV-1-elicited cytopathic effects than MT-4 cells.

Enzyme Kinetics—The chromogenic substrate Lys-Ala-Arg-Val-Nle-paranitro-Phe-Glu-Ala-Nle-amide (Sigma) was used to determine the kinetic parameters (25, 26). Wild-type protease, at final concentrations of 160–190 nM, was added to varying concentrations of substrate (100–400 μM) maintained in 50 mM sodium acetate (pH 5.0), 0.1 M NaCl, 1 mM EDTA, and assayed by monitoring the decrease in absorbance at 310 nm using a Varian Cary 100Bio UV-visible spectrophotometer. The k_{cat} and K_m values were obtained employing standard data fitting techniques for a reaction obeying Michaelis-Menten kinetics. The data curves were fitted using SigmaPlot 8.0.2 (SPSS Inc., Chicago, IL). The active enzyme concentrations were calculated from the intercept of the linear fit to the IC_{50} *versus* [S] plots with the IC_{50} axis. The K_i values were obtained from the IC_{50} values estimated from an inhibitor dose-response curve with the spectroscopic assay using the equation $K_i = (IC_{50} - [E]/2)/(1 + [S]/K_m)$, where [*E*] and [S] are the protease and substrate concentrations, respectively (27). The K_i values were measured at four to five substrate concentrations. The measurement was repeated at least three times to produce the average values.

Assay for Effects of Darunavir on Dimerized Mature Protease—To examine whether a representative dimerization inhibitor, DRV, could dissociate mature protease that had already been

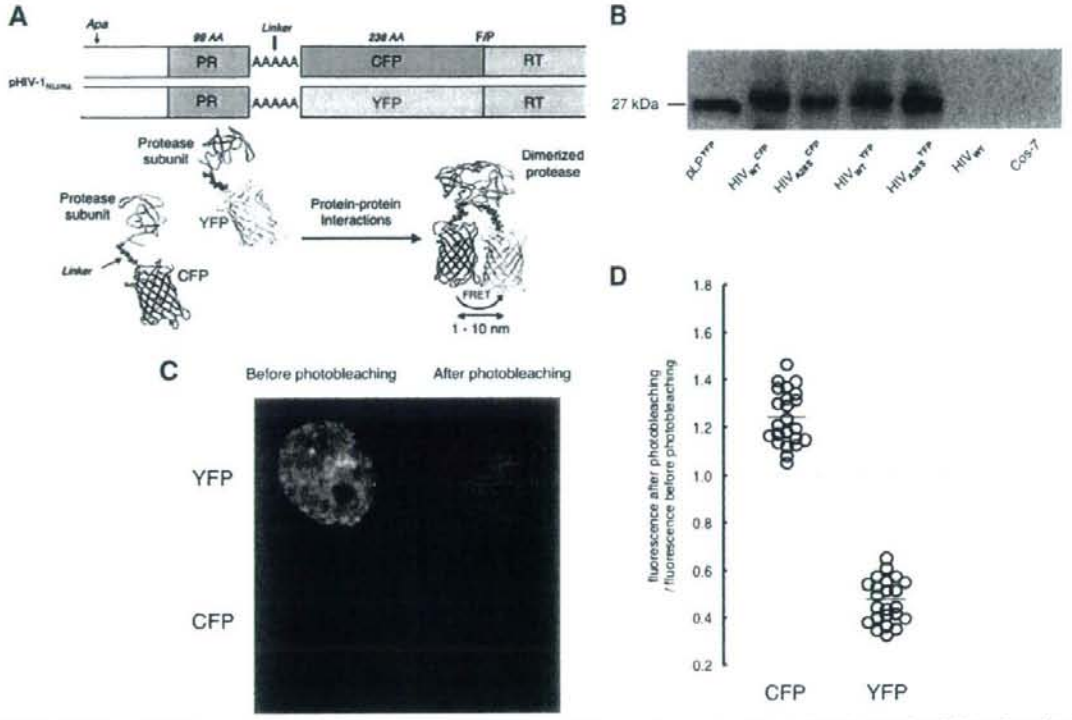

FIGURE 1. **FRET-based HIV-1 expression system.** *A*, generation of FRET-based HIV-1 expression system. Various plasmids encoding full-length molecular infectious HIV-1 (HIV-1_{NL4-3}) clones producing CFP- or YFP-tagged protease using the PCR-mediated recombination method were prepared. A linker consisting of five alanines was inserted between protease and fluorescent protein. A phenylalanine-proline site (*F/P*) that HIV-1 protease cleaves was also introduced between the fluorescent protein and RT. Shown are structural representations of protease monomers and dimer in association with the linker atoms and fluorescent proteins. FRET occurs only when the fluorescent proteins are 1–10 nm apart. *B*, expression of CFP- and YFP-tagged wild-type HIV-1 protease. To confirm the presence of HIV-1 protease tagged to fluorescent protein in COS7 cells transfected with a plasmid encoding HIV_{WT}^{CFP}, HIV_{A28S}^{CFP}, HIV_{WT}^{YFP}, or HIV_{A28S}^{YFP}, Western blot analysis was performed using lysates of pelleted virions. The CFP- and YFP-tagged proteases were visualized by SuperSignal WestPico Chemiluminescent Substrates using polyclonal anti-GFP antiserum and ECL anti-rabbit IgG peroxidase-linked species-specific whole antibody. pLP^{YFP} denotes the lysates of cells transfected with a plasmid encoding only YFP. The lysates of COS7 cells transfected with a plasmid encoding HIV_{WT}, and those of untreated COS7 cells serve as controls. *C*, fluorescence images of co-transfected cells prior to and after acceptor photobleaching. COS7 cells plated on EZ view cover-glass bottom culture plate were transfected with two plasmids, pPR_{WT}^{CFP} and pPR_{WT}^{YFP}, using Lipofectamine, cultured for 72 h, and analyzed under a Fluoview FVS00 confocal laser scanning microscope. Both PR_{WT}^{CFP} and PR_{WT}^{YFP} proteins were visualized prior to photobleaching. Note that photobleaching of the cells dramatically reduced YFP fluorescence with a $YFP^{A/B}$ ratio of 0.17 and increased CFP emission with a $CFP^{A/B}$ ratio of 1.38, signifying the dimerization of both YFP- and CFP-tagged protease subunits. *D*, ratios of the emission intensities before and after photobleaching. Fluorescence intensities of each cell transfected with two plasmids, pPR_{WT}^{CFP} and pPR_{WT}^{YFP}, were measured before and after photobleaching, and ratios of the emission intensities before and after photobleaching ($CFP^{A/B}$ ratios) were determined, and plotted. The $CFP^{A/B}$ ratio values were 1.24 ± 0.11 (n = 23), whereas the $YFP^{A/B}$ ratio values were 0.47 ± 0.09 (n = 23). The mean of these ratios are shown as *bars*.

dimerized, COS7 cells were co-transfected with a pair of plasmids encoding HIV-PR_{WT}^{CFP} and HIV-PR_{WT}^{YFP} and exposed to a protein synthesis inhibitor cycloheximide (CHX, 50 μg/ml, Sigma) at 24, 48, 72, and 96 h of culture following transfection. The cells were then exposed to DRV (1 μM) on day 5 of culture, and the values of the $CFP^{A/B}$ ratio were determined at various time points. When the $CFP^{A/B}$ ratios determined were >1.0, it was determined that HIV-1 protease had been generated and dimerization had occurred. The production of HIV-1 was monitored every 24 h following transfection by determining levels of p24 Gag protein produced into culture medium as previously described (24).

RESULTS

Generation of FRET-based HIV-1 Expression Assay—The basic concepts of the intermolecular FRET-based HIV-1-expression assay (FRET-HIV-1 assay) are shown in Fig. 1. Within a plasmid (pHIV-1_{NL4-3}), which encodes a full-length molecular infectious HIV-1 clone, the gene encoding a CFP was attached to the downstream end (C terminus) of the gene encoding an HIV-1 protease subunit through the flexible linker added (five alanines), generating pHIV-$1_{NL4-3/CFP}$ (Fig. 1*A*). Within the other plasmid (pHIV-1_{NL4-3}), the gene encoding a YFP was attached to the downstream end of protease-encoding gene in the same manner, generating pHIV-$1_{NL4-3/YFP}$. Both CFP and YFP were designed to have phenylalanine and proline in the connection with RT so that the protease is cleaved from RT when two subunits dimerize and the dimerized protease acquires enzymatic activity. Fig. 1*B* illustrates that HIV-1 virions generated in COS7 cells transfected with pHIV-$1_{NL4-3/CFP}$ contained CFP-tagged protease and those in COS7 cells transfected with pHIV-$1_{NL4-3/YFP}$ contained YFP-tagged protease as

examined in Western blotting. The HIV-1 virions produced were capable of infecting $CD4^+$ MT-4 cells when the cells were exposed to the supernatant of the transfected COS7 cells (data not shown), indicating that the expressed tagged protease was enzymatically and virologically functional. In the cytoplasm of COS7 cells co-transfected with pHIV-$1_{NL4\text{-}3/CFP}$ and pHIV-$1_{NL4\text{-}3/YFP}$, a CFP-tagged protease subunit interacts and dimerizes with a YFP-tagged protease subunit, and CFP and YFP get close because the termini are separated by only 0.5 to 1.8 nm in the dimeric form of protease (note: the representative distance was determined by analyzing the protease-DRV crystal structure (PDB ID: 2IEN)). A focused laser beam excitation of CFP (triggered by helium-cadmium laser) results in rapid energy transfer to YFP, and most of the fluorescence photons are emitted by YFP (28). If the dimerization is blocked, the average distance between CFP and YFP become larger, the energy transfer rate is decreased, and the fraction of photons emitted by YFP is lowered.

To help us interpret the energy transfer efficiency quantitatively, we used the acceptor photobleaching technique, in which the change in CFP emission quenching is measured by comparing the value before and after selectively photobleaching YFP, which prevents problems associated with variable expression levels. In this acceptor photobleaching approach, when FRET occurs, the fluorescence of the CFP donor increases after bleaching the YFP acceptor chromophore, which is recognized as a signature for FRET (18). Thus, the analysis of the change in CFP fluorescence intensity in the same specimen regions, before and after removal of the acceptor, directly relates the energy transfer efficiency to both donor and acceptor fluorescence. Fig. 1*C* illustrates representative images of co-transfected cells prior to and after YFP photobleaching, showing that, following photobleaching, YFP fluorescence of YFP-tagged wild-type protease subunit ($PR_{WT}{}^{YFP}$) was decreased, whereas CFP fluorescence of $PR_{WT}{}^{CFP}$ increased.

To further help us evaluate the energy transfer efficiency, we determined the ratios of cyan fluorescence intensity, determined with a confocal laser scanning microscope, after photobleaching over that before photobleaching (hereafter referred to as $CFP^{A/B}$ ratios). We also determined $YFP^{A/B}$ ratios in the same manner. If the $CFP^{A/B}$ ratios are >1.0, it is thought the energy transfer (or FRET) took place (18), signifying that dimerization of $PR_{WT}{}^{CFP}$ and $PR_{WT}{}^{YFP}$ subunits occurred. Fig. 1*D* shows that in the co-transfected COS7 cells (n = 23), the $CFP^{A/B}$ ratios were all >1.0 ($CFP^{A/B}$ ratios, 1.24 ± 0.11; $YFP^{A/B}$ ratios, 0.47 ± 0.09), demonstrating that dimerization of protease subunits occurred.

Changes in Fluorescence Emission with Amino Acid Substitutions in Protease—First, it was determined whether the above-described FRET-HIV-1 assay could be used to detect the disruption of HIV-1 protease dimerization. Five amino acids at the N terminus and those at the C terminus have been shown to be critical for protease dimerization (29). As shown in Fig. 2*A*, two protease monomer subunits are connected by four antiparallel β-sheets involving the N and C termini of both subunits. It is of note that mature dimerized protease has as many as 12 hydrogen bonds in this N- and C-terminal region. Thus, we introduced a Pro-1 to Ala substitution (P1A), Q2A, I3A, T4A, L5A, T96A, L97A, N98A, or F99A substitution into the replication-competent HIV-1_{NL4-3} and found that I3A, L5A, T96A, L97A, and F99A disrupted protease dimerization, although other substitutions did not disrupt the dimerization.

Several amino acid substitutions outside the N and C termini have also been known to play a role in HIV-1 protease dimerization. Ishima and Louis and their colleagues have demonstrated that the introduction of T26A, D29N, D29A, or R87K to HIV-1 protease disrupts the dimer interface contacts and destabilizes protease dimer, causing the inhibition of protease dimerization (30–32). Fig. 2 (*B* and *C*) shows the locations of intermolecular hydrogen bonds formed by such amino acids between two monomer subunits. The hydrogen bond interactions between two subunits occur between Asp-29 and Arg-8′, Arg-87 and Leu-5′, Leu-24 and Thr-26′, and Thr-26 and Thr-26′. There are also intra-molecular hydrogen bond interactions between Asp-29 and Arg-87 as shown in Fig. 2 (*B–D*). Thus, mutations in those amino acids were introduced into HIV-$PR_{WT}{}^{CFP}$ and HIV-$PR_{WT}{}^{YFP}$, generating HIV-$PR_{T26A}{}^{CFP}$, HIV-$PR_{T26A}{}^{YFP}$, HIV-$PR_{D29N}{}^{CFP}$, HIV-$PR_{D29N}{}^{YFP}$, HIV-$PR_{D29A}{}^{CFP}$, HIV-$PR_{D29A}{}^{YFP}$, HIV-$PR_{R87K}{}^{CFP}$, and HIV-$PR_{R87K}{}^{YFP}$. Co-transfection of COS7 cells with a pair of CFP- and YFP-tagged protease-carrying HIV-1-encoding plasmids demonstrated that these four amino acid substitutions disrupted protease dimerization (the average $CFP^{A/B}$ ratios were all <1.0; Fig. 2*E*). Substitutions of two amino acids adjacent to Asp-29 were also introduced, generating HIV-$PR_{A28S}{}^{CFP}$, HIV-$PR_{A28S}{}^{YFP}$, HIV-$PR_{D30N}{}^{CFP}$, and HIV-$PR_{D30N}{}^{YFP}$. Both A28S and D30N are known primary amino acid substitutions, conferring resistance to TMC126 and nelfinavir on HIV-1, respectively (33, 34). The fact that A28S- or D30N-containing HIV-1 is infectious and replication-competent indicates that these two amino acid substitutions would not disrupt protease dimerization. HIV-1 virions generated in COS7 cells transfected with HIV-$PR_{A28S}{}^{CFP}$ and HIV-$PR_{A28S}{}^{YFP}$ were confirmed to contain CFP-tagged protease and YFP-tagged protease in Western blotting, respectively (Fig. 1*B*). As expected, neither substitution disrupted the dimerization as examined in the FRET-HIV-1 assay (Fig. 2*E*). Another mutation D25A, which is adjacent to Thr^{26} and is known to abrogate replicative activity of HIV-1 (35), failed to disrupt protease dimerization, indicating that the inability of D25A mutation-carrying HIV-1 to replicate is not due to dimerization disruption, but due to the loss of proteolytic activity of dimerized HIV-1 protease. Analysis of these data indicated that the FRET-HIV-1 assay system is a reliable tool to evaluate agents for their potential to inhibit protease dimerization.

Inhibition of Protease Dimerization by Non-peptidyl and Peptidyl Compounds—After establishing the validity of the FRET-HIV-1 assay to detect protease dimerization inhibition, we evaluated various newly generated non-peptidyl small molecule agents, including the currently available anti-HIV-1 drugs for their ability to inhibit protease dimerization in a blind manner, where agents examined were identified only under code in conducting the FRET-HIV-1 assay. Six different non-peptidyl small molecule agents (GRL-0036A, GRL-06579A (26), TMC126 (33), GRL-98065 (36), DRV (24), and brecanavir (BCV) (37); M_r, ranging from 547 to 704 (Fig. 3)) were found to disrupt protease

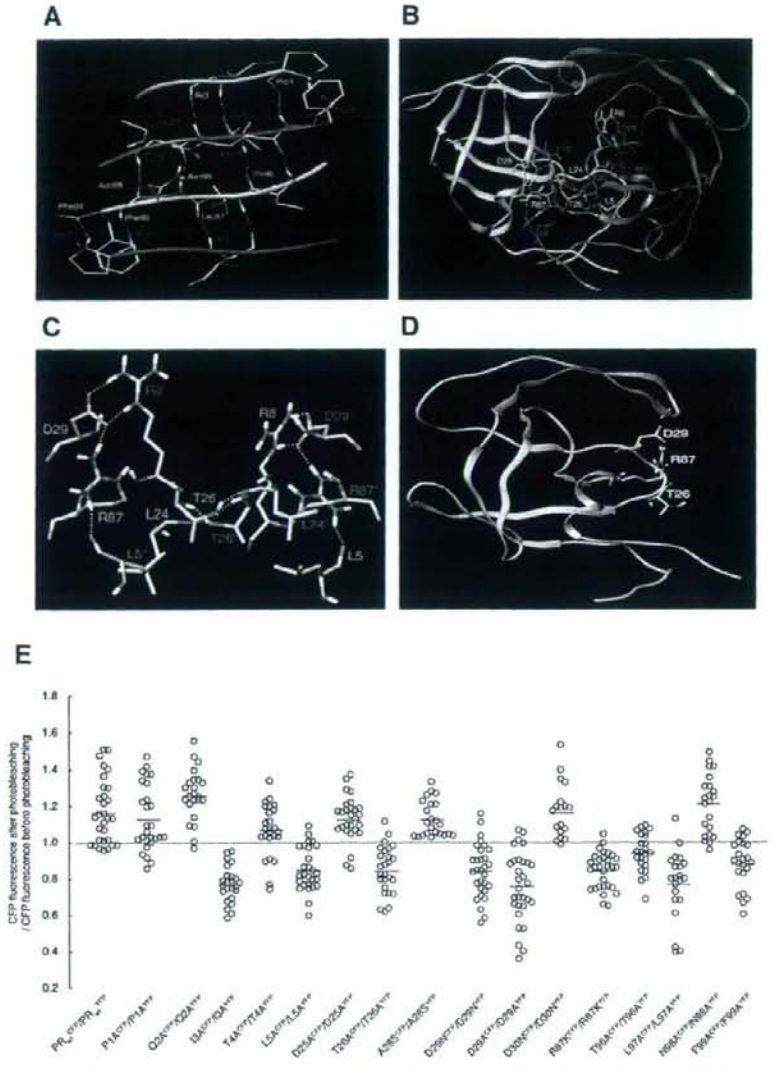

FIGURE 2. **Critical amino acid residues for protease dimerization.** *A*, four antiparallel β-sheets involving the N and C termini of both monomer subunits. Two HIV-1 protease monomer subunits are connected by four antiparallel β-sheets involving the N and C termini of both monomer subunits. It is of note that mature dimerized protease has as many as 12 hydrogen bonds in this N- and C-terminal region, and these interactions seem to be critical for dimer formation. A monomer subunit is shown by the *green ribbon*, and the other monomer subunit is shown by the *red ribbon*. A molecule disrupting these inter-protease hydrogen bond contacts can also disrupt their dimerization. *B* and *C*, intermolecular hydrogen bonds between two HIV-1 protease monomer subunits. The figure shows the intermolecular hydrogen bonds between two protease monomer subunits. The hydrogen bond interactions between protease monomer A (shown as *green ribbon*) and monomer B (shown in *red ribbon*) are Asp-29 to Arg-8′, Arg-87 to Leu-5′, Leu-24 to Thr-26′, and Thr-26 to Thr-26′. The corresponding amino acids of monomer B also form hydrogen bonds with monomer A (*i.e.* Asp-29′ to Arg-8, etc.). Intra-molecular hydrogen bond interaction between Asp-29 and Arg-87 is shown by *white dotted lines*. The residues forming critical intermolecular contacts between two monomer subunits are shown by atom color types (C, *gray*; N, *blue*; O, *red*; and H, *white*). Only polar hydrogens are shown. The residues of chain A are labeled *green*, and those of chain B are labeled *red*. This provides a structural explanation to the FRET experimental data, which show that mutations Leu-5, Asp-29, Thr-26, and Arg-87 prevent formation of a protease dimer. *D*, potential binding sites of the small molecule dimerization inhibitors. The figure shows one of the potential binding sites of the dimerization inhibitors. Asp-29, Arg-87, and Thr-26 are spatially close enough to form binding interactions with the dimerization inhibitor and prevent the other protease monomer from interacting with these residues. *E*, changes in emission intensity ratios upon amino acid substitution. COS7 cells were co-transfected with a pair of HIV-PR^{CFP} and HIV-PR^{YFP} carrying wild-type protease or protease with one amino acid substitution, and CFP$^{A/B}$ ratios were determined. The CFP$^{A/B}$ ratio value for $PR_{WT}{}^{CFP}/PR_{WT}{}^{YFP}$ was 1.17 ± 0.18 (mean ± S.D.); $PR_{P1A}{}^{CFP}/PR_{P1A}{}^{YFP}$, 1.13 ± 0.18; $PR_{Q2A}{}^{CFP}/PR_{Q2A}{}^{YFP}$, 1.26 ± 0.14; $PR_{T3A}{}^{CFP}/PR_{T3A}{}^{YFP}$, 0.77 ± 0.10; $PR_{T4A}{}^{CFP}/PR_{T4A}{}^{YFP}$, 1.07 ± 0.14; $PR_{L5A}{}^{CFP}/PR_{L5A}{}^{YFP}$, 0.85 ± 0.12; $PR_{D25A}{}^{CFP}/PR_{D25A}{}^{YFP}$, 1.13 ± 0.12; $PR_{T26A}{}^{CFP}/PR_{T26A}{}^{YFP}$, 0.84 ± 0.13; $PRA_{28S}{}^{CFP}/PR_{A28S}{}^{YFP}$, 1.13 ± 0.10; $PR_{D29N}{}^{CFP}/PR_{D29N}{}^{YFP}$, 0.84 ± 0.15; $PR_{D29A}{}^{CFP}/PR_{D29A}{}^{YFP}$, 0.76 ± 0.19; $PR_{D30N}{}^{CFP}/PR_{D30N}{}^{YFP}$, 1.17 ± 0.15; $PR_{R87K}{}^{CFP}/PR_{R87K}{}^{YFP}$, 0.84 ± 0.10; $PR_{T96A}{}^{CFP}/PR_{T96A}{}^{YFP}$, 0.94 ± 0.10; $PRL_{97A}{}^{CFP}/PR_{L97A}{}^{YFP}$, 0.77 ± 0.19; $PR_{N98A}{}^{CFP}/PR_{N98A}{}^{YFP}$, 1.21 ± 0.16; and $PR_{F99A}{}^{CFP}/PR_{F99A}{}^{YFP}$, 0.88 ± 0.13. All the experiments were conducted in a blind fashion. The CFP$^{A/B}$ ratio that is >1 signifies a protease dimer, whereas a ratio that is <1 signifies disruption of protease dimerization. Note that the residue (such as Ile-3 or Asp-29) whose mutation resulted in disruption of dimerization had an inter-molecular hydrogen bond contact with the other protease monomer as shown in *A–C*. The mean value of the ratios is shown as *bars*.

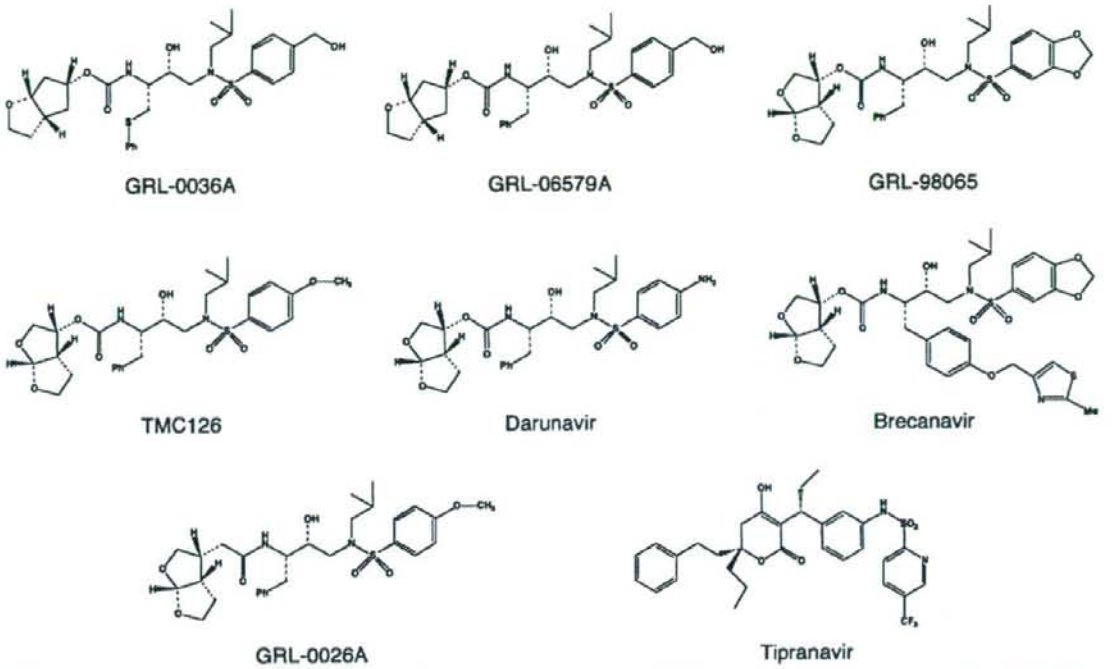

FIGURE 3. **Structures of dimerization inhibitors identified.** Structures of eight dimerization inhibitors are shown. The IC_{50} values for activity against HIV-1 in acute HIV-1 infection assays are shown in Table 1.

dimerization at concentration of 1 μM in the assay (Fig. 4*A*). All of these agents had potent inhibitory activity against HIV-1 protease with K_i values of 29, 3.5, 10, 14, 16, and 6.8 pM, respectively, as examined in the assay previously described (25, 26), and were highly potent against HIV-1_{LAI} in acute HIV-1 infection assays using target $CD4^+$ MT-2 cells (24) with IC_{50} values of 0.0002–0.005 μM (Table 1). In addition to small molecule agents, we examined various peptides in the FRET-HIV-1 assay. A 27-amino acid peptide containing the dimer interface sequences amino acids 1–5 and amino acids 95–99 (P27: PQITLRKKRRQRRRPPQVSFNFATLNF), which blocks HIV-1 infectivity and replication (14), also inhibited protease dimerization as examined in the FRET-HIV-1 expression assay. Another peptide P9 (RKKRRQRRRPPQVSFNF) that lacks the dimer interface sequences and is not active against HIV-1 (14) failed to inhibit protease dimerization in the FRET-HIV-1 assay. These data again corroborated the utility of the assay to evaluate protease dimerization.

To test the robustness and reproducibility of the FRET-HIV-1 assay data, we determined the $CFP^{A/B}$ ratios in a total of 143 COS7 cells transfected with $pPR_{WT}{}^{CFP}$ and $pPR_{WT}{}^{YFP}$ plasmids and cultured in the presence or absence of 1 μM DRV for 3 days on 11 different occasions. In the presence of DRV, only 7 (4.9%) of 143 cells had the ratios of slightly more than 1.0, whereas all the rest (95.1%) had values of <1.0 ($n = 143$; average of 0.73 ± 0.22) (Fig. 4*B*). The $CFP^{A/B}$ ratios determined in the absence of DRV were mostly >1.0 ($n = 172$, average of 1.21 ± 0.17). We next examined whether a dose response in the dimerization inhibition could be seen when the cells were exposed to various concentrations of DRV. As shown in Fig. 4*C*, DRV effectively inhibited protease dimerization at concentrations of 0.1 μM and above, whereas the average $CFP^{A/B}$ ratio was slightly >1.0 at 0.01 μM, and no dimerization inhibition was seen at 0.001 μM. These data show that the inhibition by DRV was roughly dose-responsive up to 0.1 μM. In addition, we examined a TMC126-congener GRL-0026A (Fig. 3) that is substantially less potent than TMC126 against HIV-1 with IC_{50} of 0.48 μM (Table 1), along with TMC126 and BCV for their dose response dimerization inhibition in the FRET-HIV-1 assay and found that the inhibition was similarly dose-responsive (Fig. 4*D*).

None of the FDA-approved Anti-HIV-1 Drugs Except TPV Blocks Dimerization—We asked whether other currently approved PIs blocked protease dimerization in the FRET-HIV-1 assay. None of the seven PIs (saquinavir, nelfinavir, amprenavir, indinavir, ritonavir, lopinavir, and atazanavir) inhibited protease dimerization at 1 μM concentration, whereas the control DRV clearly inhibited the dimerization as shown in Fig. 4*E*. Considering that DRV is generally more potent against HIV-1 *in vitro* than most currently existing PIs (24), four PIs (saquinavir, amprenavir, nelfinavir, and atazanavir) were examined in the FRET-HIV-1 assay at a higher concentration, 10 μM, however, none of these four PIs inhibited protease dimerization (Fig. 4*F*). Interestingly, TPV, which has been shown to provide more favorable virological and immunological responses in patients who have received extensive previous antiretroviral treatment than an optimized background regimen when